7-1997

Relative Motion between the Caribbean and North American Plates and Related Boundary Zone Deformation from a Decade of GPS Observations

Timothy H. Dixon
University of Miami, thd@usf.edu

Frederic Farina
University of Miami

Charles DeMets
University of Wisconsin

Pamela Jansma
University of Puerto Rico

Paul Mann
University of Texas at Austin

See next page for additional authors

JOURNAL OF GEOPHYSICAL RESEARCH, VOL. 103, NO. B7, PAGES 15,157–15,182, JULY 10, 1998

Relative motion between the Caribbean and North American plates and related boundary zone deformation from a decade of GPS observations

Timothy H. Dixon,[1] Frederic Farina,[1] Charles DeMets,[2] Pamela Jansma,[3] Paul Mann[4] and Eric Calais[5]

Abstract. Global Positioning System (GPS) measurements in 1986, 1994, and 1995 at sites in Dominican Republic, Puerto Rico, Cuba, and Grand Turk define the velocity of the Caribbean plate relative to North America. The data show eastward motion of the Caribbean plate at a rate of 21 ± 1 mm/yr (1 standard error) in the vicinity of southern Dominican Republic, a factor of 2 higher than the NUVEL-1A plate motion model prediction of 11 ± 3 mm/yr. Independent measurements on San Andres Island, and an Euler vector derived from these data, also suggest a rate that is much higher than the NUVEL-1A model. Available data, combined with simple elastic strain models, give the following slip rate estimates for major left-lateral faults in Hispaniola: (1) the North Hispaniola fault offshore the north coast of Hispaniola, 4 ± 3 mm/yr; (2) the Septentrional fault in northern Dominican Republic, 8 ± 3 mm/yr; and (3) the Enriquillo fault in southern Dominican Republic and Haiti, 8 ± 4 mm yr. The relatively high plate motion rate and fault slip rates suggested by our study, combined with evidence for strain accumulation and historical seismicity, imply that seismic risk in the region may be higher than previous estimates based on low plate rate/low fault slip rate models and the relatively low rate of seismicity over the last century.

1. Introduction

One of the important discoveries in the last decade was the recognition that the velocities of Earth's major lithospheric plates, as measured by marine magnetic anomalies averaged over several million years or predicted by plate motion models based on these and other data [e.g., *DeMets et al.*, 1990], are equivalent, within small uncertainties, to velocities measured by independent space geodetic techniques over 5 to 10 years, including satellite laser ranging [*Smith et al.*, 1990; *Robbins et al.*, 1993; *Cazenave et al.*, 1993], very long baseline interferometry [*Robaudo and Harrison*, 1993], and the Global Positioning System [*Argus and Heflin*, 1995; *Dixon and Mao*, 1997; *Larson et al.*, 1997]. This equivalence is generally interpreted not only as an indication of the steadiness of plate motion over several million years but also, with some circularity, as validation of both the space geodetic techniques and the models. However, a complete test of this equivalence remains to be done. For logistical and economic reasons the space geodetic sites used in these pioneering studies necessarily omitted several plates, including the Caribbean plate. This is a critical omission because the velocity of this plate with respect to its neighbors is poorly known on both geologic and geodetic timescales.

While there has been much research on this topic using global models [*Jordan*, 1975; *Stein et al.*, 1988; *DeMets et al.*, 1990] and models based on local earthquake slip vectors [*Sykes et al.*, 1982; *Deng and Sykes*, 1995], large uncertainties remain, reflecting complex regional geology. Transform fault azimuths, earthquake slip vectors, mid-ocean ridge spreading rates, and other relative motion indicators are poorly defined, inconsistent, sparse, or nonexistent around the boundary of the Caribbean plate. Most parts of this boundary are actually broad, deforming zones of continental or transitional arc continental crust, complicating interpretation of kinematic indicators. The most poorly determined Euler vectors in global plate motion models such as NUVEL-1 and 1A [*DeMets et al.*, 1990, 1994] generally involve the Caribbean plate, reflecting these problems.

This paper reports the first geodetic measurements of Caribbean plate motion. We use Global Positioning System (GPS) data acquired in several experiments spanning up to a decade to derive a velocity estimate and uncertainties for the Caribbean plate. We also discuss implications for strain partitioning and earthquake hazard in the northeastern Caribbean. Although our data are too sparse to develop a detailed picture of strain distribution, we can put broad constraints on the slip rates of major faults in Hispaniola, and assess the influence of elastic

[1]Rosenstiel School of Marine and Atmospheric Sciences, University of Miami, Miami, Florida.

[2]Department of Geology and Geophysics, University of Wisconsin, Madison.

[3]Department of Geology, University of Puerto Rico, Mayaguez.

[4]Institute of Geophysics, University of Texas at Austin.

[5]Institut de Geodynamique, Centre National de la Recherche Scientifique, Varrieres-le-Buisson, France.

Paper number 97JB03575.

0148-0227/98/97JB-03575$09.00

strain accumulation on measured site velocities for the purpose of estimating plate motion. We show that some plate motion is likely accommodated offshore north of Hispaniola, that the Enriquillo fault in southern Hispaniola accomodates more plate motion than is generally assumed, that the geodetic velocity of the Caribbean plate relative to North America is about twice as fast as the NUVEL-1A model prediction, and that the velocity difference is statistically significant at 95% confidence. To our knowledge this is the first major discrepancy between this plate motion model and a direct geodetic measurement.

2. Data Acquisition, Analysis, and Quality Assessment

GPS data were acquired at sites in Cuba, Dominican Republic, and Puerto Rico as well as North America (Figure 1) in campaigns in 1986, 1994, and 1995, as part of a series of observations we have termed the Caribbean-North America Plate Experiment (CANAPE). We also report a velocity for a permanent GPS station installed on St. Croix in 1995, and a velocity for a site on San Andres island in the Caribbean plate interior based on campaigns in 1991, 1994, and 1996. Data collection and analysis procedures evolved considerably over the ten years spanning these observations. Because the resulting differences can impact accuracy, we review in this section the important aspects of data acquisition in the various campaigns, analytical procedures for these disparate data, and methods to assess accuracy. Readers interested primarily in geological implications may wish to skip to section 3.

2.1. Data Acquisition

Four Caribbean plate sites were occupied in June 1986. These are Isabella (ISAB) on the island of Puerto Rico and three sites in Dominican Republic on the island of Hispaniola: Cabo Francis Viejo (FRAN), Capotillo (CAPO), and Cabo Rojo (ROJO) (Table 1 and Figure 1).

Table 1. Sites and Observation Epochs for the Caribbean-North American Plate Experiment

Site	Latitude, °N	Longitude, °W	1986[a]	1994[a]	1995[a]	Description
		Caribbean Plate				
ANDR (3009-S)[b]	12.53	81.73	-	-	-	San Andres Island
CAPO (3004-S)	19.42	71.67	6	6	-	Capotillo
COLO (3269-S)	18.37	71.45	-	5		La Colonia Mixta
CONS (3265-S)	18.92	70.77	-	5	-	Constanza
CRO1[c]	17.76	64.58	-	-	C	St. Croix
CUMB (3266-S)	19.51	70.51	-	7	-	La Cumbre
ESCO	18.32	71.57	-	4	-	Puerto Escondido
FRAN (3003-S)	19.67	69.94	7	6	2	Cabo Frances Viejo
GORD	18.43	64.44	-	5	-	Virgin Gorda
ISAB (3005-S)	18.47	67.05	7	6	2	Isabela
JUAN (3268-S)	18.81	71.24	-	6		San Juan De La Maguana
MOCA (3267-S)	19.38	70.53	-	5	-	Moca
PARA	17.97	67.04	-	5	-	Parguera
ROJO (3002-S)	17.90	71.67	6	5	2	Cabo Rojo
SANA (3039-S)[b]	12.52	81.73	-	-	-	San Andres Island
SCRX (USCGS LAMB)	17.76	64.57	-	5	2	St. Croix
SDOM (3040-S)	18.47	69.88	-	10	-	Santo Domingo
SOSU (3264-S)	19.75	70.58	-	6	-	Sosua
VEGA (3263-S)	19.30	70.57	-	5	-	La Vega
		North American Plate[d]				
GTMO (3001-S)	19.90	75.12	6	6	-	Guantanamo
RICH (Timer 1962)	25.61	80.38	7	-	-	Richmond
RCM5[c]	25.61	80.38	-	C	C	Richmond
TURK (Laser 1975)	21.46	71.13	7	6	4	Grand Turk

Characters in parentheses after site names are monument inscriptions.

[a] Numbers indicate days of data at this site at listed epoch used in this study; dashes indicate site was not occupied.

[b] ANDR occupied for 8 days in February 1991; SANA occupied for 5 days in February 1991, 12 days in February 1994 and 3 days in February 1996 as part of Central and South American experiment [*Kellogg and Dixon*, 1990].

[c] Permanent, continuously (C) recording site.

[d] Caribbean region only.

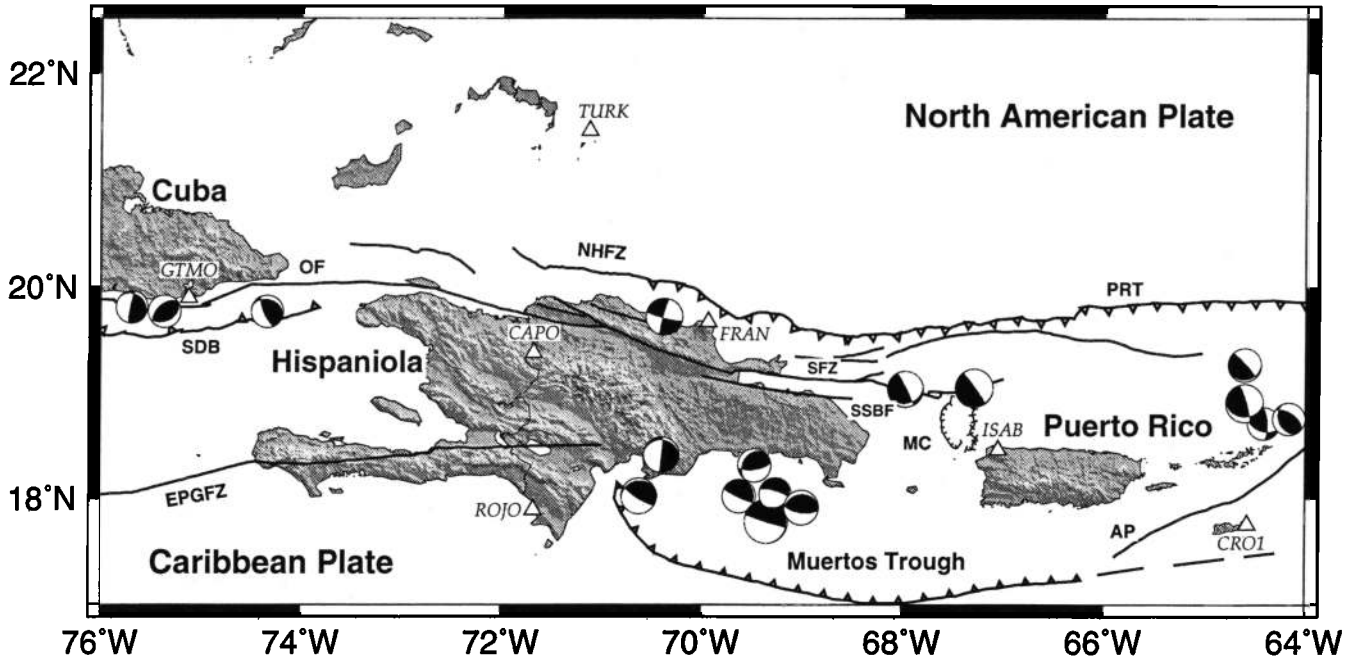

Figure 1. Major faults, other tectonic features, earthquakes, and Global Positioning System (GPS) site locations (open triangles, four letter site names) in the northeastern Caribbean, superimposed on shaded relief topography. AP is Anegada Passage, EFZ is Enriquillo fault zone, MC is Mona Canyon, NHFZ is North Hispaniola fault zone, OF is Oriente Fault, PRT is Puerto Rico Trench, SDB is Santiago Deformed Belt, SFZ is Septentrional Fault Zone, SSBF is South Samana Bay Fault. Island of Hispaniola includes Haiti (west of border) and Dominican Republic (east of border). Earthquakes are from Harvard Centroid Moment Tensor catalogue [*Dziewonski and Woodhouse*, 1983] and show all available events shallower than 50 km (17 events between 1979 and 1992). Event clusters near 69°W and 64°W displaced slightly for clarity. Fault map is modified from *Case and Holcombe* [1980], *Calais and Mercier de Lepinay* [1991], *Mann et al.* [1991], *Masson and Scanlon* [1991], and *Dolan and Wald* [1997].

These sites were reoccupied in May-June 1994, along with additional sites to densify the network. In November 1995 we were able to reoccupy only a small number of sites, returning to the original 1986 sites, except CAPO, which could not be observed. Observations on the island of St. Croix (SCRX) were made in May-June 1994 and November 1995. In November 1995 a permanent GPS station was installed in St. Croix at a new site (CRO1), about 1 km away from our original site. The velocity estimate for San Andres Island, Colombia, is based on observations at two sites (SANA and ANDR) in February 1991, February 1994, and February 1996, part of the Central and South America project [*Kellogg and Dixon*, 1990].

Several North American plate sites were occupied in 1986, including Richmond, Florida (RICH), near Miami; Grand Turk, Turk, and Caicos Islands (TURK); and Guantanamo Bay, Cuba (GTMO), plus several sites on the mainland United States for satellite tracking and reference frame definition (Table 1). By 1994, data from many additional North American and global sites were available from permanent GPS stations, eliminating the need for "custom" occupation of specific sites in North America, save those of geologic significance for this project (TURK and GTMO). The new permanent sites differ from the original 1986 sites, but in several cases they are close, and accurate vector ties are available to link the two time series where necessary (Table 2). GTMO was not observed in 1995.

Table 1 summarizes locations, monument names, monument inscriptions, and occupation histories of each site. Here we report velocities for all sites occupied in at least two campaigns; most velocities are based on data from three campaigns separated by at least 5 years. Velocities for CAPO and GTMO are based only on the 1986 and 1994 campaigns. St. Croix's velocity is based on observations in 1994 and 1995 at the U.S. Coast and Geodetic Survey station LAMB (SCRX in our analysis), supplemented by continuous data from the new permanent station CRO1 beginning just before our 1995 campaign. We combined the two data sets using a vector tie between the sites, estimated from 2 days of simultaneous observations in 1995. The resulting tie (Table 2) is the weighted mean of the 2 days and allows us to define the velocity of a single "pseudosite" (referred to as CRO1) over a period greater than 2 years. Similarly, for San Andres we combined the data using the weighted mean of 4 days of simultaneous occupation in 1991.

The 1986 data were acquired with TI-4100 receivers sampling at 2-min intervals. The same kind of receivers were sent to several tracking sites in North America (Table 1) for reference frame definition and improvement of satellite orbit estimates. These receivers tracked up to four Block - 1 satellites for approximately 8 hours per day. Although limited in data volume by the four-channel restriction and the small number of satellites and tracking stations available at that time, the 1986 data are nevertheless relatively high in quality: dual - frequency P code

Table 2. Vector Site Ties

Site	Monuments	X, m	Y, m	Z, m	Reference[a]
Richmond, Florida	Timer 1962 (RICH)[b] to RCM5	16.985	-19.303	-28.608	1, 2
Hat Creek, California	7218 to NCMN-B[b]	97.9746	-73.5856	33.4897	1
Ft. Davis, Texas	7900 to Harvard RM4 1977[b]	36.0961	3.2117	20.3152	1
Haystack/Westford Massachusetts	7091 to OCP-3[b]	-43.695	-11.544	3.256	3
St. Croix, US Virgin Islands	LAMB to CRO1[c]	-926.560	-534.578	-291.768	4
San Andres Island, Colombia	SANA to ANDR[d]	415.1947	156.3506	619.6819	4

See Table 1 for site abbreviations. Add listed values to coordinates of first site to obtain coordinates of second site.

[a] References: 1, *Bryant and Noll* [1993]; 2, International Earth Rotation Service; 3, National Geodetic Survey/HAVAC 82.06.2; 4 this study (see text).

[b] Site used in 1986.

[c] LAMB was occupied in 1994 and 1995 only. CRO1 is a permanent site that began observations in late 1995.

[d] ANDR was occupied in 1991 with a Trimble SST. SANA was occupied in 1991 (Trimble SST), 1994 (Turborogue), and 1996 (Trimble SSE).

pseudorange and carrier phase data were recorded, uncorrupted by either anti-spoofing (A/S) or selective availability (S/A). The 1994 and 1995 CANAPE data were acquired with Trimble SSE receivers sampling at 30-s intervals. Block - 2 satellites were available for observation by these eight-channel receivers, significantly increasing data volume. Both A/S and S/A affected the signals recorded during the 1994 and later observations but did not significantly impact accuracy given current observation and analysis procedures. We typically included 12-14 globally distributed tracking stations in our analyses of the 1994 and 1995 data to improve the reference frame definition (Table 3). All of the stations used in this capacity were equipped with TurboRogue receivers, Dorn Margolin antennas, and "choke ring" style back planes. Table 1 does not list the tracking stations used in analysis of the 1994 and later data because a large number are available and results are not sensitive to the exact number or distribution of these stations assuming global coverage is achieved.

Table 3. Difference (rms) between International Terrestrial Reference Frame 1994 (ITRF-94) and this Solution at Colocated Sites

Date	Number of Sites	North, cm	East, cm	Vertical, cm
May 25, 1994	12	2.4	2.1	5.2
May 26, 1994	15	0.8	1.6	2.5
May 27, 1994	12	2.5	3.1	2.8
May 28, 1994	8	1.8	3.3	4.3
May 31, 1994	14	2.5	2.9	5.1
June 01, 1994[a]	12	3.6	1.6	5.8
Nov 06, 1995	12	1.3	1.8	2.9
Nov 07, 1995	12	3.1	1.9	3.4
Nov 09, 1995	13	1.9	2.1	3.5

Root-mean-square values of residual vectors for north, east, or vertical component are given, where residual is the difference between our solution and ITRF-94 on a given day.

[a] Data are anomalous compared with the other 5 days of 1994 observations and were not used in the coordinate velocity estimates.

The permanent station at St. Croix uses a TurboRogue receiver and Dorn - Margolin antenna, sampling at 30-s intervals. It became operational in October 1995. Thus the tie and the resulting augmented time series represent data acquired with two different receiver/antenna systems.

Data from San Andres Island were collected with a Trimble SST receiver in 1991, a TurboRogue receiver in 1994, and a Trimble SSE receiver in 1996, all sampling at 30-s intervals.

2.2. Data Analysis

Results from the 1986 campaign were presented by *Dixon et al.* [1991a]. For this paper the 1986 data were reanalyzed using updated software and models. Analysis procedures for the 1994 and 1995 data are described by *Dixon et al.* [1997]. Briefly, we used the GIPSY software [*Lichten*, 1990] developed at the Jet Propulsion Laboratory (JPL), incorporating precise satellite ephemerides and clock files provided by JPL based on analysis of data from a

global network of GPS stations [*Zumberge et al.*, 1997]. The ephemerides we use are not fixed to a specific reference frame, but our analysis includes a number of sites (typically about a dozen; Table 3) whose positions are defined in a current realization of the International Terrestrial Reference Frame (ITRF), in this case, ITRF-94 [*Boucher et al.*, 1996]. A transformation is carried out using these colocated sites and the sites of interest following procedures outlined by *Blewitt et al.* [1992] and *Heflin et al.* [1992], placing the estimated positions of the Caribbean and North American sites as well as the tracking sites in ITRF-94. The difference between the estimated positions of the sites based on our data and the defined positions of the tracking sites in ITRF-94 is one measure of the consistency of our global reference frame definition, typically several centimeters (Table 3). The three-dimensional deviation between the observed (our solution) and predicted (ITRF-94) values is dominated by the vertical component (average rms deviation 3.7 cm) which is not important for this study. The average north and east rms deviations are 2.0 and 2.4 cm, respectively (Table 3).

2.2.1. Orbit estimation for 1986 data. Analysis procedures for the 1986 data differed in several important ways. For these data the relevant satellite ephemerides and clock files are not available from JPL (or, to our knowledge, anywhere else), nor are there sufficient globally distributed tracking data available to follow the "no-fiducial" approach outlined above. We therefore estimated our own satellite ephemerides and clock files for these data, fixing the locations of three "tracking" sites in North America to their ITRF-94 positions in order to define a reference frame.

The tracking stations available for 1986 data are Westford, Massachusetts; Richmond, Florida; Fort Davis, Texas; and Hat Creek, California (Table 2). We fixed Westford, Ft. Davis and Hat Creek for all days where these three stations were available, estimating the positions of Richmond and all remaining stations. If data from one of the three primary stations were unavailable, Richmond was fixed instead. Data from these days were not used to estimate Richmond's velocity.

Tracking data from additional sites not listed above were collected in the 1986 experiment, some of which were incorporated in earlier analyses [*Dixon et al.*, 1991a]. Unfortunately, not all these data were available for this more recent analysis because they were not archived, the archive is not known to us, the original nine-track tapes had degraded, or critical ancillary data such as site logs with antenna heights were not archived with the raw GPS data. Fortunately, the currently accessible data are adequate for our purposes, as demonstrated below. The data used in this study are now archived at National Science Foundation's UNAVCO facility in Boulder, Colorado, and are publicly available.

Two of the 1986 tracking sites (Richmond and Fort Davis) have their positions and velocities defined in the ITRF-94. However, two other stations (Westford and Hat Creek) have only positions defined; their velocities are not defined in this version of the ITRF [*Boucher et al.*, 1996]. Since we require knowledge of these sites' positions at epoch 1986 rather than 1993 (ITRF-94 site positions are defined for epoch 1993), we first need an accurate velocity estimate for Westford and Hat Creek consistent with the remaining stations and the reference frame as a whole. We estimated this in two ways. For Hat Creek we used the ITRF-93 velocity [*Boucher et al.*, 1994] with an empirical correction, estimated from the difference between ITRF-93 and ITRF-94 velocities at Quincy, a tracking site about 100 km southeast of Hat Creek whose velocity is defined in both reference frames. For Westford, we used the Euler vector derived by *Dixon et al.* [1996], based on a least squares fit to the ITRF-94 velocities of eight stations on the stable interior of North America, to predict Westford's velocity. An independent very long baseline interferometry (VLBI) derived velocity in ITRF-94 yields a similar result (Z. Altamimi, written communication 1997).

The "fiducial" approach (three fixed stations) used for 1986 data should yield position estimates equivalent to the no-fiducial approach used for later data as long as the locations of the three fixed sites are consistent and well defined in the ITRF-94 and the GPS data are of high quality. Any error in the assumed locations of these sites, in their ITRF-defined velocities, in the site tie information, or in the GPS data acquired at these sites in 1986 will translate into an error in the Caribbean site position estimates for that epoch, biasing the resulting velocity estimates. Given the different procedures described above for determining ITRF-94 velocities, the various ties used, and the generally lower quality of the early observations, we need a way to assess the quality of the 1986 results, particularly the fidelity of the tracking network and its influence on site velocities. One approach is to use various combinations of available tracking stations and look at consistency. Since we have four tracking stations available and only three are required to define the reference frame, we can test four different combinations.

Figure 2a compares results for the four possible fiducial networks in 1986 using the TURK-ROJO baseline as an example, as it measures Caribbean-North America relative motion. The change in relative position caused by different tracking site combinations, a measure of systematic error introduced by fiducial station mislocation and GPS observation error at these stations, is much smaller than day-to-day scatter, a measure of random and possibly systematic error from other effects. Since the fiducial error is smaller than the other errors, we conclude that our approach to orbit estimation and reference frame definition for the 1986 data is adequate for baselines (relative positions) in the Caribbean data set.

Figures 2b and 2c show the scatter in the "absolute" position coordinates (ITRF-94 coordinates) for the same two stations. Here the overall scatter is greater, with scatter due to different fiducial networks on a given day almost as large as day to day scatter. This reflects the fact that orbit and reference frame errors do not cancel when absolute position coordinates are estimated, unlike the relative position coordinates (Figure 2a). This implies that coordinate velocities (Tables 5 and 6b) incorporating the 1986 data will be noisier compared with baseline velocities (Table 6a) from the same data.

2.2.2. Resolution of carrier phase cycle ambiguities. The precision of our GPS position estimates depends on the ability to make precise phase measurements on the two GPS carrier signals, with wavelengths of about 19 and 24 cm. However, to derive the final position estimates, it is also necessary to estimate

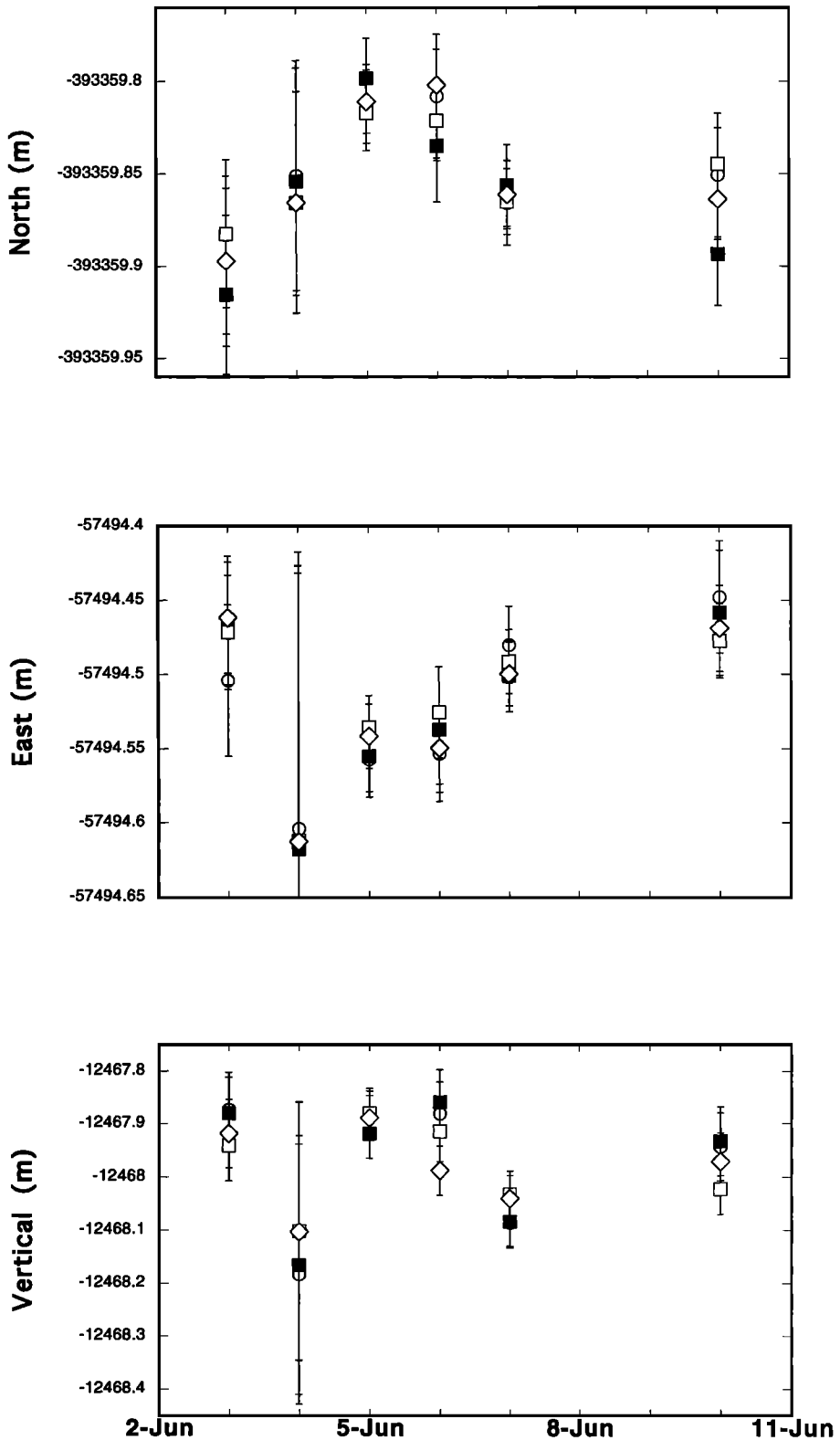

Figure 2a. Coordinates of Cabo Rojo (ROJO) relative to Grand Turk, Turks and Caicos Islands (TURK) in 1986 for various combinations of fiducial networks (fixed stations). Diamonds indicate Richmond, Haystack, and Hat Creek are fixed in the analysis; circles indicate Richmond, Hat Creek and Fort Davis are fixed; open squares indicate Richmond, Haystack, and Fort Davis are fixed; solid squares indicate Haystack, Hat Creek and Fort Davis are fixed.

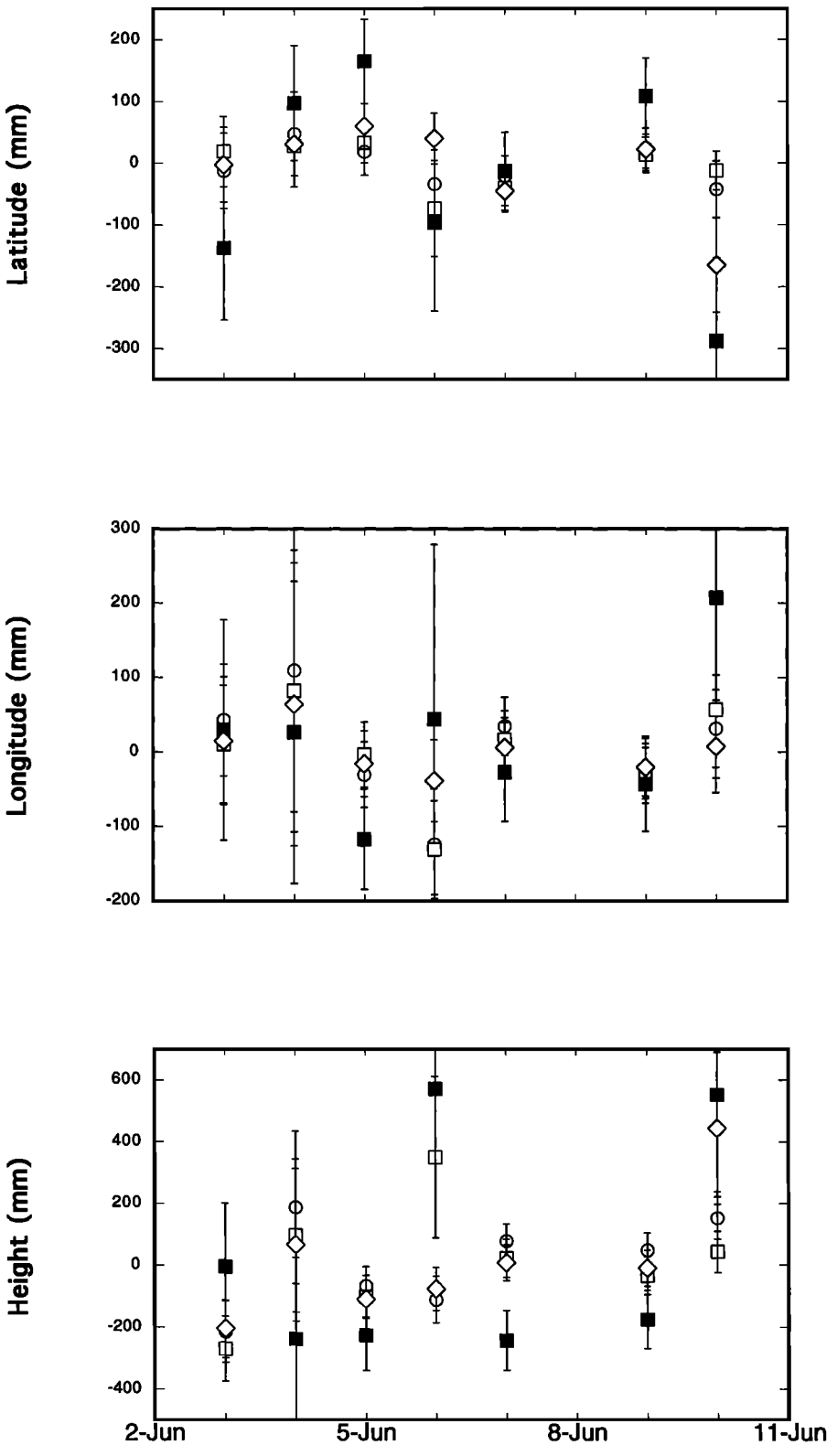

Figure 2b. "Absolute" (ITRF-94) coordinates for TURK for various combinations of fiducial networks (fixed stations). Symbols same as Figure 2a.

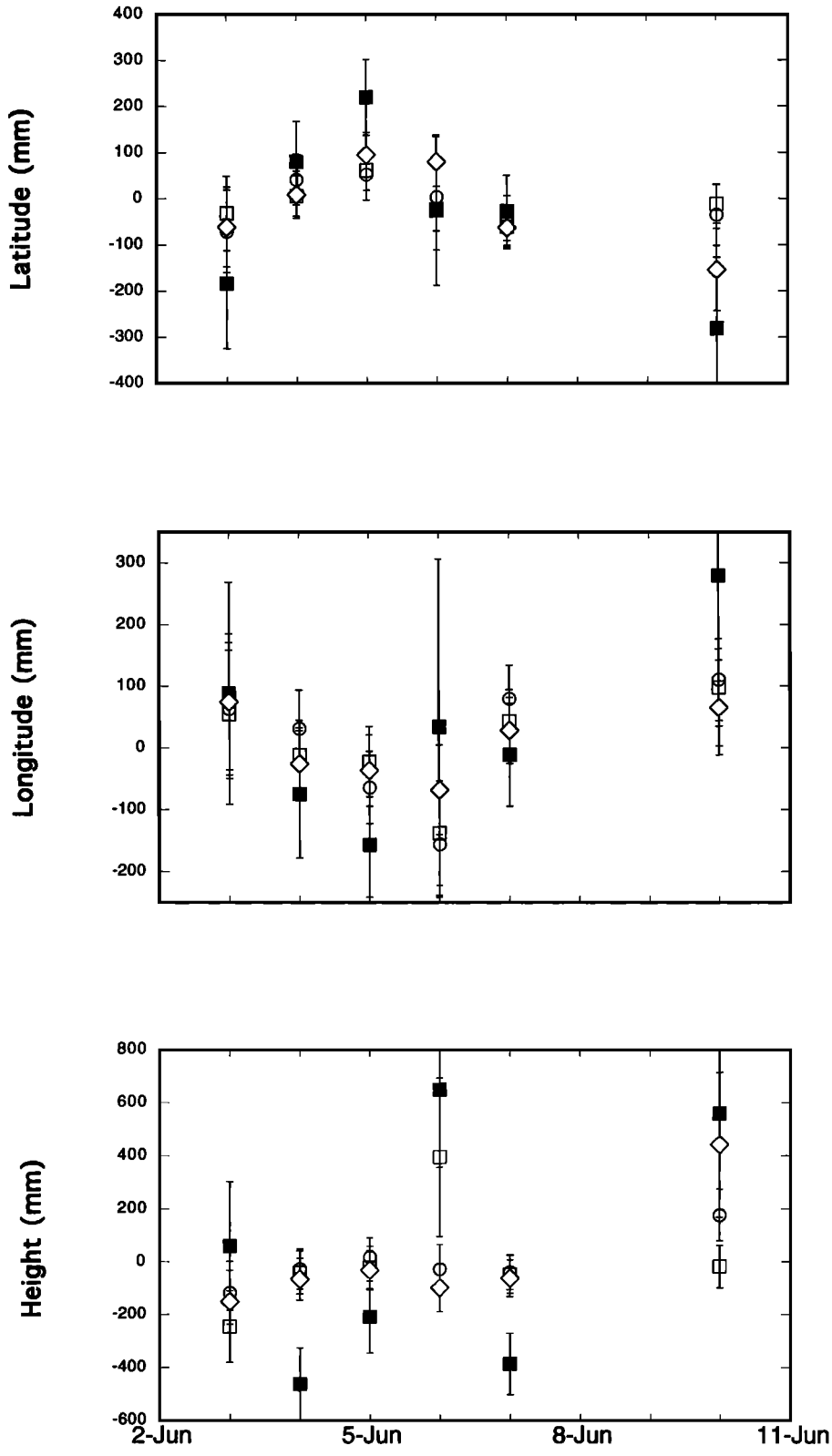

Figure 2c. "Absolute" (ITRF-94) coordinates for ROJO for various combinations of fiducial networks (fixed stations). Symbols same as Figure 2a.

the total number of cycles between the satellite transmitter and ground receiver at some time. This quantity is usually estimated as a real number. Alternately, we can exploit the integer nature of this quantity along with geometric constraints to strengthen the estimate. This resolution of carrier phase cycle ambiguities (bias fixing) can reduce the scatter in the position and velocity estimates, especially for the east component. On the other hand, if the carrier phase bias is inadvertently fixed to the wrong integer value, a significant error can result. We used a fairly stringent statistical criterion (99% confidence) before fixing a bias to an integer value, which, on some days, meant that less than 50% of the biases were successfully resolved (remainder estimated as real numbers). For one day (May 26, 1994) we were unable to resolve a significant number of biases. Table 4 compares bias-fixed and bias-free estimates for the velocity of ROJO relative to TURK. The two results are equivalent at 95% confidence, but the bias-fixed result has a lower scatter in the horizontal components. Except for Figure 2 and the bias-estimated entry in Table 4, all the CANAPE data discussed in this paper are bias-fixed. Lack of geometric constraints for isolated sites such as San Andres Island or the global tracking sites precludes resolution of their carrier phase biases with our current software. For these data the carrier phase biases are estimated as real numbers.

2.3. Site Velocities and Errors

Site velocities (Tables 4-8) are based on weighted least squares fits to the daily position data, with weights based on the inverse variance ($1/\sigma^2$, where σ is the formal error of the daily position estimates). The formal error includes the effect of data weighting and total observing time on a given day, and is scaled (usually upward) to reflect day to day scatter, such that χ^2 per degree of freedom is 1.0 for the linear model. The rate uncertainties listed in the various tables (1 standard error) depend on the scaled formal error of the daily position estimates, the total time span of observations (usually 9.4 years), and our estimate of time-correlated error (see below). The estimated velocities are sensitive to errors in the 1986 data. These data are noisier than later data, and given the temporal spacing of observations, strongly influence the slope of the best fit line on a position vs time plot.

In the presence of time-correlated noise, velocity errors calculated assuming only white noise (that is, each position measurement is independent, and errors are uncorrelated from one measurement epoch to the next) underestimate the true velocity error [*Johnson and Agnew*, 1995]. *Dixon et al.* [1997] studied 2.5 years of length data between two sites spanning the resurgent dome in Long Valley Caldera, California, and found that horizontal velocity errors were underestimated by factors of 2-4 if time-correlated errors were ignored. *Zhang et al.* [1997] studied 19 months of data from ten sites in southern California and found that velocity errors were underestimated by factors of 2-6 if time-correlated errors were ignored. Here we are mainly concerned with long-term temporal correlations with respect to the observation epoch (e.g., 8 days in 1986). While short-term correlations may be present, the scatter and scaled formal error should largely reflect the resulting variation as long as the characteristic time scale of the error is shorter than the observation epoch. With limited data it may be difficult to distinguish white noise from short-term, time-correlated noise.

Table 4. Bias-Estimated and Bias-Fixed Velocity Estimates for ROJO relative to TURK

	North, mm/yr	East, mm/yr	Vertical, mm/yr
Estimated	-2.2 ± 1.1	24.0 ± 1.6	2.4 ± 3.2
Fixed	0.3 ± 0.8	20.6 ± 1.0	-1.6 ± 4.0

Errors are one standard error, based on white noise approximation.

Spurious monument motion ("ground noise") has been modeled as a random walk process, a type of time-correlated noise [*Johnson and Agnew*, 1995]. *Langbein and Johnson* [1997] studied time series of precise, two-color Electronic Distance Measurement (EDM) data in California, and found random walk values of 0.5-4.0 mm/√yr. *Dixon et al.* [1997] used a value of 2 mm/√yr to account for random walk monument noise associated with a short (8 km) baseline, where orbit and reference frame errors are negligible. Monument noise presumably afflicts all our CANAPE site velocities but is probably significant only for relative positions, where orbit and other errors are minimized. We added 2 mm/√yr to the error estimates of all our CANAPE baseline velocities (e.g., Table 6a), which inflates the velocity error estimates by about 0.2-0.3 mm/yr compared to the white noise-only assumption.

Other sources of time-correlated noise are probably more important for GPS and include unmodeled satellite accelerations, reference frame effects, and seasonal or annual environmental effects. Orbit and reference frame errors especially impact the coordinate solutions, where common mode errors do not cancel as they do for relative positions (see section 2.4). Environmental effects may also be important in the Caribbean and include low frequency multipath or signal scattering that varies with soil moisture or moisture on the antenna element or ground plane, and unmodeled gradients in atmospheric water vapor that could vary over time (our analysis assumes azimuthal symmetry at all times and thus mismodels this behavior). *Dixon et al.* [1991a] found the wet tropospheric path delay in the 1986 Caribbean GPS data to be both high and highly variable, implying that this could be a significant noise source in these and later Caribbean data, and modeled the delay as a random walk. *Dixon and Kornreich Wolf* [1990] observed wet delay gradients in Costa Rica with water vapor radiometers. *Chen and Herring* [1997] found significant atmospheric gradient effects in VLBI data. *MacMillan et al.* [1997] observed atmospheric gradients with VLBI data from St. Croix and noted velocity effects at about the 1 mm/yr level. Our GPS data are analyzed only above 15° elevation, where the effect of atmospheric gradients in reduced compared with the 5°-10° elevation cutoff typical for VLBI. However, because of differing sensitivities to gradients for the two techniques, we cannot preclude GPS velocity errors at about the 1 mm/yr level due to mismodeling of tropospheric asymmetry.

Zhang et al. [1997] found that time-correlated noise in GPS data from southern California could be modeled as flicker noise or fractal white noise, with less power in the

low frequency domain compared with random walk noise. They were able to exploit the dense GPS network available in this region, removing a common mode error from the time series prior to noise analysis [*Wdowinski et al.*, 1997]. This common mode error is probably dominated by orbit error and is likely present in our coordinate solutions as well. Lacking a dense permanent network, this approach is not feasible for the Caribbean region, hence the nature and magnitude of our time-correlated noise could differ significantly from the California example. For simplicity we modeled the time-correlated noise in our coordinate solutions as a random walk, calculating an additional error term added in quadrature to the white noise rate error estimate:

$$V^v_{tot} = V^v_{wht} + V^v_{rwk} \quad (1)$$

where V^v_{tot} is the velocity variance $(\sigma^v)^2$ and the subscripts refer respectively to total variance, white noise variance, and random walk variance. The random walk variance is just $(\sigma^v_{rwk})^2 / T$, where T is the total time span of observations. Equation (1) is only an approximation but, given other uncertainties, is probably adequate. To estimate σ^v_{rwk}, we used 3.0 years of continuous data from a permanent GPS station at Richmond, Florida, a subtropical site that may be representative of Caribbean conditions, and applied maximum likelihood estimation [*Langbein and Johnson,* 1997], which in this case assumes that a time series has both white and random walk components. We obtained random walk noise estimates of 8.2 ± 1.5, 10.6 ± 1.0, and 10.3 ± 2.5 mm/√yr for the north, east, and vertical components, respectively, within the range of values reported by *Zhang at al.* [1997]. If time-correlated noise is better represented by a process with lower spectral index [*Zhang et al.*, 1997], this procedure may overestimate the velocity error. On the other hand, our random walk noise model, while adequately representing orbit error in 1994 and later data, underestimates orbit error in the 1986 data, and thus might underestimate total velocity error. Application of our random walk noise model has the effect of inflating coordinate velocity errors of CANAPE sites by 0.7-1.7 mm/yr compared with white noise only estimates. The effect is small and insensitive to the exact value assigned to random walk noise because of the long time span of observations (T=9.4 yr). The error estimates for SANA and CRO1 are affected by larger amounts (up to 4 mm/yr; compare Figures 4 and 5 with Table 5), reflecting their shorter occupation histories (T=5.0 and 3.3 yrs respectively). In section 2.4 we describe several tests for consistency involving internal comparisons, and one comparison with independent data, which suggest that our error estimates are reasonable, if somewhat ad hoc.

2.4. Benchmark Ties

Table 2 lists the vectors used in this study to connect position time series from different benchmarks at the same general location. Two of these (St. Croix and San Andres Island) were generated as part of this study. Figure 3 shows the velocity of CRO1, using data combined from the two St. Croix sites. If we use only the 2.0 years of data available from the permanent station, we obtain horizontal

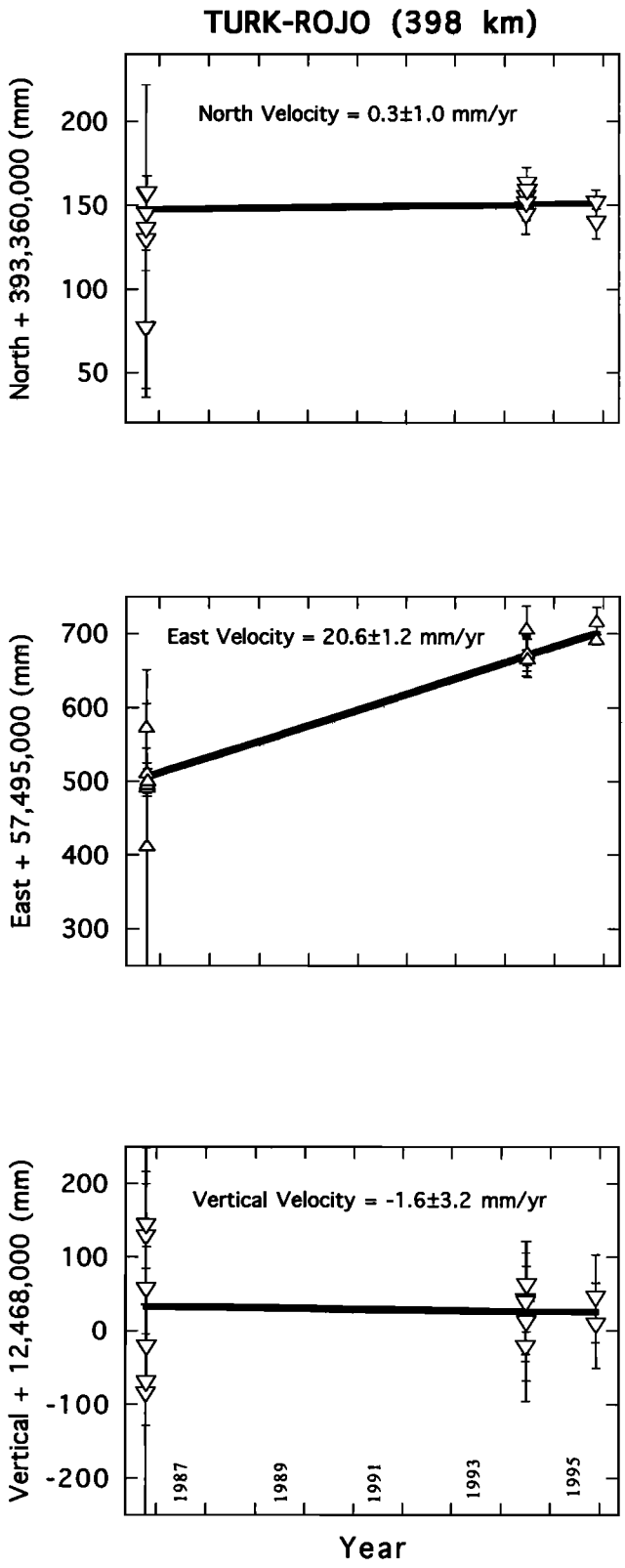

Figure 3. Daily solutions for ITRF-94 coordinates at St. Croix. Error shown on plot is scaled white noise only. Total error, with random walk noise added in quadrature to white noise, is listed in Table 5. Data beginning late 1995 were acquired at the new St. Croix site, CRO1. Data in mid-1994 and 2 days in late 1995 were acquired at site SCRX (Table 1), about 1 km away, and are added to plot via a vector tie (Table 2) based on the 2 days of simultaneous observations in late 1995.

velocities that are virtually identical (within 0.1 mm/yr) to the combined data set, while the two vertical velocities differ slightly, but by less than the uncertainty: 11.9 ± 1.6 mm/yr (2.0 years) versus 11.3 ± 1.6 mm/yr (combined data) (errors based on white noise only). Different antennas were used at each end of this short baseline, a Trimble antenna with flat ground plane at SCRX and a Dorn-Margolin antenna with choke ring back plane at CRO1. Although a nominal phase center offset is employed in our analysis for each antenna, we have not corrected for different elevation angle-dependent behavior of the two antennas.

Figure 4 shows the combined data for the two sites on San Andres Island, ANDR and SANA. Here the two data sets are indistinguishable in all three components, perhaps reflecting the longer time span of simultaneous data to define the tie (4 versus 2 days) and the fact that the tie was made with identical receiver-antenna systems at each end of the short baseline. In summary, the tie information is believed to be accurate at the several millimeter level or better and to cause negligible velocity error.

2.5. Local and Regional Reference Frames

One aim of our study is to define the velocity of Caribbean sites relative to the North American plate for comparison to other data and models. Simultaneous GPS measurements at one or more sites on stable North America are helpful in this regard. Data from many such sites are available for 1994 and later CANAPE observations and for 1991 and later SANA observations. However, in 1986, only a few tracking sites were occupied; of these, an even smaller number (Richmond, Grand Turk, Westford, and

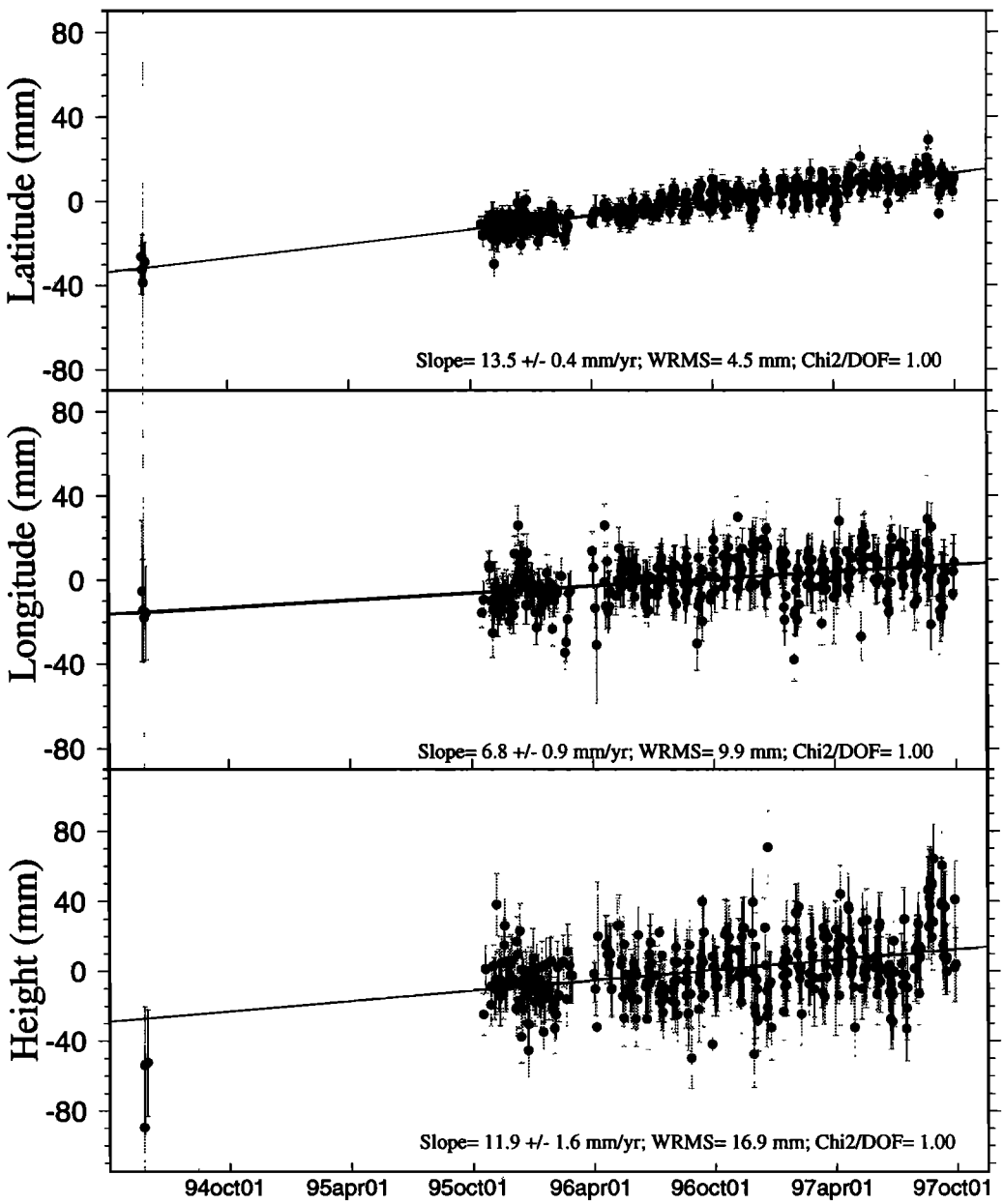

Figure 4. Similar to Figure 3, available daily solutions at the San Andres Island site (SANA). Data in 1991 were acquired at sites SANA and ANDR (Table 1), about 650 m apart. ANDR data added with vector tie (Table 2) based on 4 days of simultaneous observations in 1991. Data in 1994 and 1996 were acquired at SANA.

Fort Davis) were located on the stable craton. Grand Turk is the only site reoccupied in all three CANAPE campaigns.

The inherent rigidity of the North American plate, the spatial extent of the North American GPS data, and the accuracy of the individual site velocities (both Caribbean and North American) all influence the accuracy of Caribbean site velocities referenced to North America. It is important not only to define our North American reference frame in an optimum way, but also to assess the influence of uncertainties in this reference frame on the resulting relative velocity estimates.

Argus and Gordon [1996] used a decade of VLBI data to investigate the stability of plates including cratonic North America and concluded that most plates, including North America, were rigid to better than 2 mm/yr. *Dixon et al.* [1996] used 2 years of GPS data to study the rigidity of cratonic North America and found that the average velocity deviation from a rigid plate model for eight sites was 1.3 mm/yr, while the maximum deviation was 2.3 mm/yr. In the latter study, since deviations from the rigid plate model include GPS velocity errors as well as any nonrigid plate process, the residuals likely reflect an upper limit for the rigidity of cratonic North America. These studies suggest that our ability to define velocities of Caribbean sites relative to North America is not limited by nonrigidity of the North American plate, but rather by GPS observation errors.

We use the available GPS data to define stable North America in two independent ways and report two corresponding sets of results. The agreement (or lack) between the two is a good test of data consistency. First, we report site velocities relative to TURK, which we term a local reference frame. This site is several hundred kilometers north of the Caribbean-North American plate boundary, on a stable carbonate platform at the southern end of the Bahamas Banks (Figure 1). The entire region is tectonically inactive, and should be geologically equivalent to stable North America. The same monument was occupied in all three campaigns, eliminating site tie uncertainties as a noise source. Postglacial rebound, a measurable effect at some reference sites in North America, is also negligible. Finally, the baselines are short enough (baselines between TURK and the three Hispaniola sites are all less than 400 km long) that orbit errors affect sites at each end of the baseline in a similar way and largely cancel. *Dixon et al.* [1991a] discuss the magnitude of this effect. Reduction of orbit errors is especially important for the 1986 data, which lack a strong satellite tracking network. Disadvantages of this approach are that results are sensitive to observation errors at a single station (TURK), and possible rigid body rotations about a vertical axis near TURK (e.g., a rotation of the reference frame) could impart a relative velocity to the Caribbean sites unrelated to the signal of interest. Also we require simultaneous observations at each end of the baseline, which can impose logistical difficulties. While it is possible to define a relative position (baseline) without simultaneous observation, there is little advantage in doing so, as there is no cancellation of common mode errors. Thus we do not define the velocity of CRO1 relative to TURK since most of the observations are not simultaneous. Figure 5 shows the daily position estimates for the ROJO-TURK baseline, representative of the other baselines and important for defining Caribbean-North American velocity. Table 6a and Plate 1 summarize the velocities of all the Caribbean sites and GTMO with respect to TURK.

Second, we define a regional reference frame using data from a widely dispersed set of permanent GPS stations on stable North America [*Dixon et al.*, 1996] (Tables 5 and 6b; Plate 1). To ensure that the two reference frames are independent, we exclude TURK from the reference frame inversion, treating it as a site whose velocity we wish to estimate relative to stable North America, and providing an independent test of its stability. The advantages of this approach are that Caribbean site velocities are not sensitive to rigid body rotations, except the Caribbean-North American plate velocity of interest, and there is reduced sensitivity to noise at any one North American station.

Unfortunately, there is a major disadvantage in terms of noise at the Caribbean sites. Modern coordinate velocities from a sparse network of continuously operating GPS stations can be applied to plate motion studies even with as little as 2 years of data [*Dixon et al.*, 1996; *Dixon and Mao*, 1997]. The success of this approach derives from the relatively high accuracy of post-1992 GPS orbit and site coordinate solutions, coupled with the large amount of data available from a continuously operating station, which allows rapid reduction of white noise through $1/\sqrt{n}$ averaging, where n is the number of data (observation days). However, coordinate velocities and the corresponding regional reference frame approach are less useful for campaign style data such as CANAPE, where sparse data limit averaging of white noise, and pre-1992 data suffer from much higher orbit uncertainties. Thus the regional reference frame velocities (Table 6b) have higher uncertainties compared with the local reference frame velocities (Table 6a; Plate 1). Most of our discussions therefore focus on the more precise local reference frame results. The regional reference frame results are nevertheless important, as they provide an independent test of TURK's stability as a reference site and some indication (within rather large errors) of the effects of local rotations.

2.6. Reliability of Velocity and Error Estimates

We tested the sensitivity of the velocity estimates to observations at any one epoch, focusing on the two sites whose velocity may approximate the stable interior of the Caribbean plate, ROJO and SANA. This procedure also tests the error estimates: if the velocity estimate of any data subset differs significantly from another or from the whole (i.e., more than the listed error), it might suggest that some systematic error not reflected in our error bars is affecting one or more observations. Table 7a lists the velocity of ROJO relative to TURK based on the three data subsets (1986-1994, 1986-1995, and 1994-1995) and the complete data set. The velocities are all equivalent within 1 standard error. The velocity based on just the 1994-1995 pair has the largest error. Even though the 1994 and 1995 data are high in quality and more precise than the 1986 data, the short time span between the two epochs (17 months) precludes precise velocity estimates. The older data, despite larger scatter, are important for defining precise site velocities. Table 7b lists the corresponding

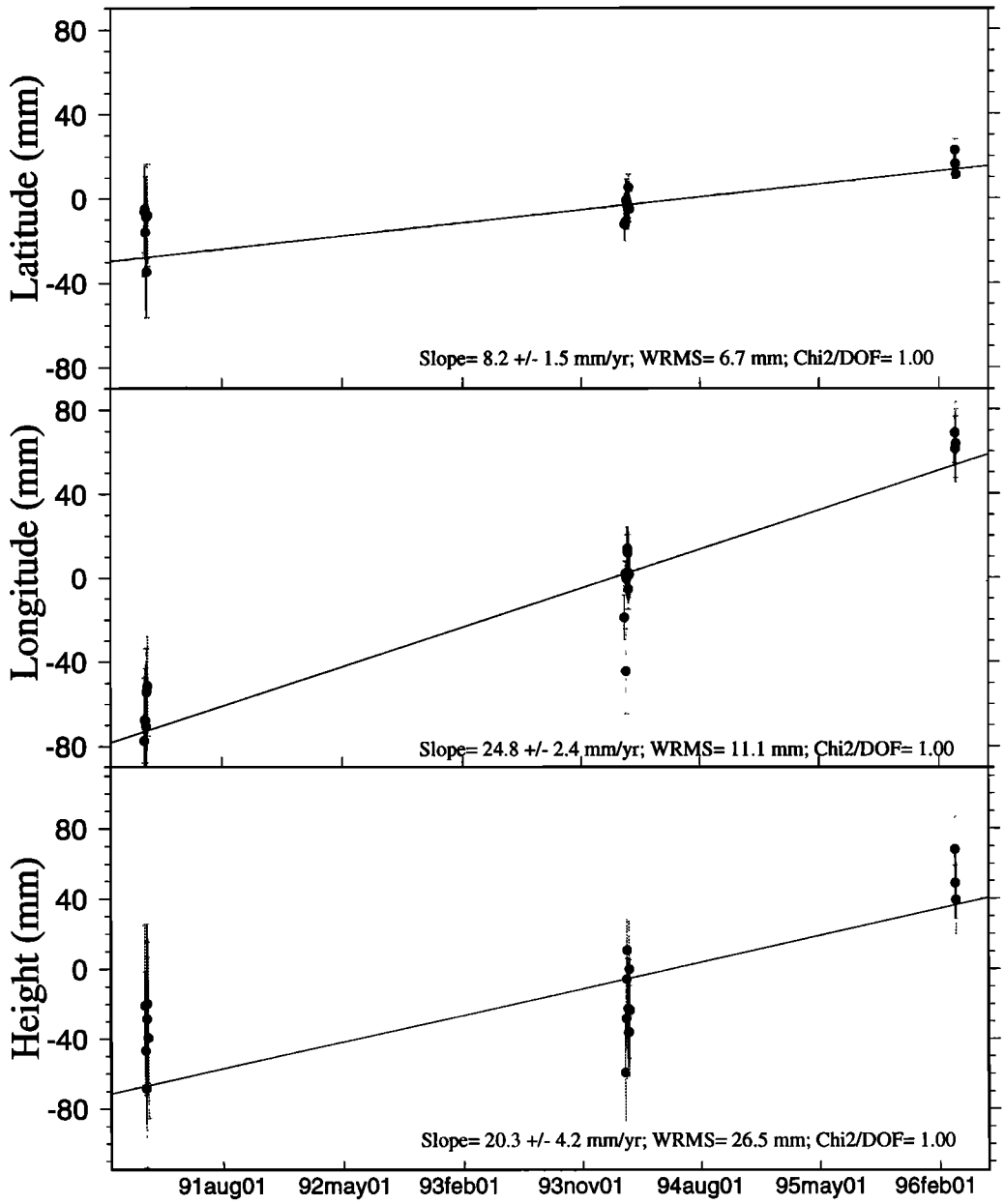

Figure 5. Position of TURK relative to ROJO based on simultaneous observations at each site in 1986 (6 days), 1994 (5 days), and 1995 (2 days). Listed velocity and error (1 standard error) are based on weighted least squares, straight line fit, scaled white noise plus random walk noise (2.0 mm/√yr) model. For 1986 east component data, note cluster of 4 data points near 500 mm.

velocities for SANA, using the four possible combinations of observations in 1991, 1994, and 1996. Again, the velocity based on the shortest time span (1994-1996) has the largest error, and almost all the velocities based on the data subsets are equivalent to the full data set within 1 standard error; all are equivalent within 2 standard errors.

VLBI data spanning 4 years (1993-1997) are available at St. Croix [*MacMillan et al.*, 1997] allowing comparison of a Caribbean GPS site velocity with an independent technique. The velocities from the two techniques are equivalent within 1 standard error (Table 8).

Inspection of the velocity data in Figures 3-5, Plate 1, and Tables 4-8 suggests several important points that bear on data quality and error estimation:

1. Relative position estimates plotted as a function of time (Figure 5, as well as other baseline plots not shown) define a nearly linear set of points spanning almost 10 years. This suggests that a constant velocity model is appropriate, that our analysis procedures for treating the disparate data sets are adequate, and that in cases where only two site occupations are available (GTMO and CAPO; See Table 1) the velocity estimates are reasonable, if somewhat noisier.

2. TURK's velocity with respect to the regional North American reference frame is 0 within 2 standard errors (95% confidence), validating its use as a reference station and proxy for stable North America in the local reference frame.

Table 5. Velocities of Caribbean and Selected North American Sites in ITRF-94

	North, mm/yr	East, mm/yr	Vertical, mm/yr
	Caribbean Plate Sites		
CAPO	5.0 ± 3.4	6.6 ± 5.2	1.6 ± 7.7
FRAN	6.1 ± 3.9	-5.6 ± 5.1	0.6 ± 7.1
ISAB	5.5 ± 4.8	10.0 ± 5.8	-3.5 ± 6.9
ROJO	5.0 ± 3.9	12.3 ± 5.9	3.5 ± 7.5
SANA[a]	8.2 ± 4.2	24.8 ± 6.5	20.3 ± 8.5
CRO1[a]	13.5 ± 4.5	6.8 ± 5.9	11.9 ± 5.9
	North American Plate Sites[b]		
GTMO	5.1 ± 2.9	-3.2 ± 4.6	-3.7 ± 8.3
TURK	2.8 ± 3.7	-10.8 ± 4.5	-0.2 ± 5.1

Uncertainties are one standard error, based on a model with white measurement noise and random walk noise added in quadrature. Random walk estimates based on data from Richmond, Florida (see text). Table 1 gives station abbreviations.

[a] Bias-estimated solution.

[b] Caribbean region only.

3. Site velocities in the two reference frames are equivalent (Tables 6a and 6b) within 2 standard errors for all sites. Most velocity components overlap at 1 standard error.

4. In both the local and regional reference frames, vertical component velocities for all sites differ insignificantly from 0 at 2 standard errors; most sites differ insignificanly from 0 at 1 standard error. Expected vertical rates for known tectonic processes in the region are less than a few millimeters per year, consistent with the observations and error estimates.

5. VLBI and GPS velocities for St. Croix relative to stable North America agree within 1 standard error.

6. The various velocity estimates based on data subsets overlap within quoted uncertainties, suggesting that we have not underestimated the velocity errors.

3. Results And Discussion

Our major results are summarized by the site velocities (Tables 6a and b) and the corresponding velocity map (Plate 1). These data provide new information on the overall direction and rate of Caribbean plate motion and on some tectonic processes in the northeastern Caribbean, including strain partitioning, block rotation, and elastic strain accumulation. These topics are not independent. We first assess the effects of elastic strain and block rotation on measured site velocities. Based on this, we suggest that some of our sites approximate the stable Caribbean plate interior, derive an Euler vector describing Caribbean-North America motion, and discuss implications for the direction and rate of Caribbean plate motion.

3.1. Elastic Strain Accumulation and Strain Partitioning

There is a southward increase in site velocities in Dominican Republic (Plate 1). This linear velocity gradient might reflect several processes, including (1) the cumulative effect of aseismic creep and seismic strain accumulation along numerous small faults within a broad zone of shear, each fault accommodating a fraction of the total plate rate; (2) the effect of elastic strain accumulation on one or a few locked faults, with the corresponding "slip deficit" to be made up in the future in one or more large earthquakes. Occasional large earthquakes, the mapped presence of a few major faults, lack of direct observation of fault creep in the area, and the fit of a simple elastic model to available data (see below) are all consistent with a model involving elastic strain accumulation on a few major faults, and we make that assumption in the remainder of this paper.

We can assess, and to first order correct for, elastic strain accumulation. This allows us to compare decade scale, intraseismic geodetic velocities with long-term geologic average slip rates that span many earthquake cycles. In this approach, we assume that the measured site velocities reflect the long-term geologic slip rate on one to several faults modified only by elastic strain accumulation, ignoring, for example, possible effects of postseismic viscoelastic relaxation [*Pollitz*, 1992]. This latter process is potentially important in Dominican Republic, given the timing and magnitude of the 1946 *Ms* = 7.8 north coast earthquake, an oblique slip earthquake with a significant thrust component [*Russo and Villasenor*, 1995, 1997; *Dolan and Wald*, 1997], but is beyond the scope of this report.

Hispaniola marks a restraining bend in an otherwise east-west trending transform boundary [*Mann and Burke*,

Table 6a. Velocity of Caribbean Sites and Guantanomo Relative to Grand Turk

	North, mm/yr	East, mm/yr	Vertical, mm/yr
CAPO	-1.5 ± 0.8	11.6 ± 1.0	-0.4 ± 3.8
FRAN	1.6 ± 0.8	4.9 ± 1.0	-1.1 ± 3.9
GTMO	-1.9 ± 0.8	6.9 ± 1.4	-2.3 ± 4.8
ISAB	5.5 ± 1.5	19.4 ± 1.3	-5.9 ± 3.0
ROJO	0.3 ± 1.0	20.6 ± 1.2	-1.6 ± 4.5

Uncertainties are 1 standard error, based on a model with white measurement noise and random walk monument noise (2.0 mm/√yr) added in quadrature.

Table 6b. Velocity of Caribbean and Selected North American Sites Relative to Stable North America

	North, mm/yr	East, mm/yr	Vertical, mm/yr
CAPO	1.1 ± 3.4	11.6 ± 5.3	1.6 ± 7.7
CRO1	6.9 ± 4.5	10.9 ± 6.0	11.9 ± 5.9
FRAN	1.5 ± 3.9	-0.6 ± 5.2	0.6 ± 7.1
GTMO	2.5 ± 2.9	2.0 ± 4.7	-3.7 ± 8.3
ISAB	-0.2 ± 4.8	14.5 ± 5.9	-3.5 ± 6.9
ROJO	1.1 ± 3.9	16.7 ± 6.0	3.5 ± 7.5
SANA	8.2 ± 3.9	27.2 ± 5.4	20.3 ± 6.2
TURK	-1.4 ± 3.7	-5.1 ± 4.6	0.2 ± 5.1

Uncertainties are 1 standard error. Velocities and errors are based on values in Table 5, and defined by minimizing in a least squares sense the velocities of eight sites on stable North America [*Dixon et al.*, 1996].

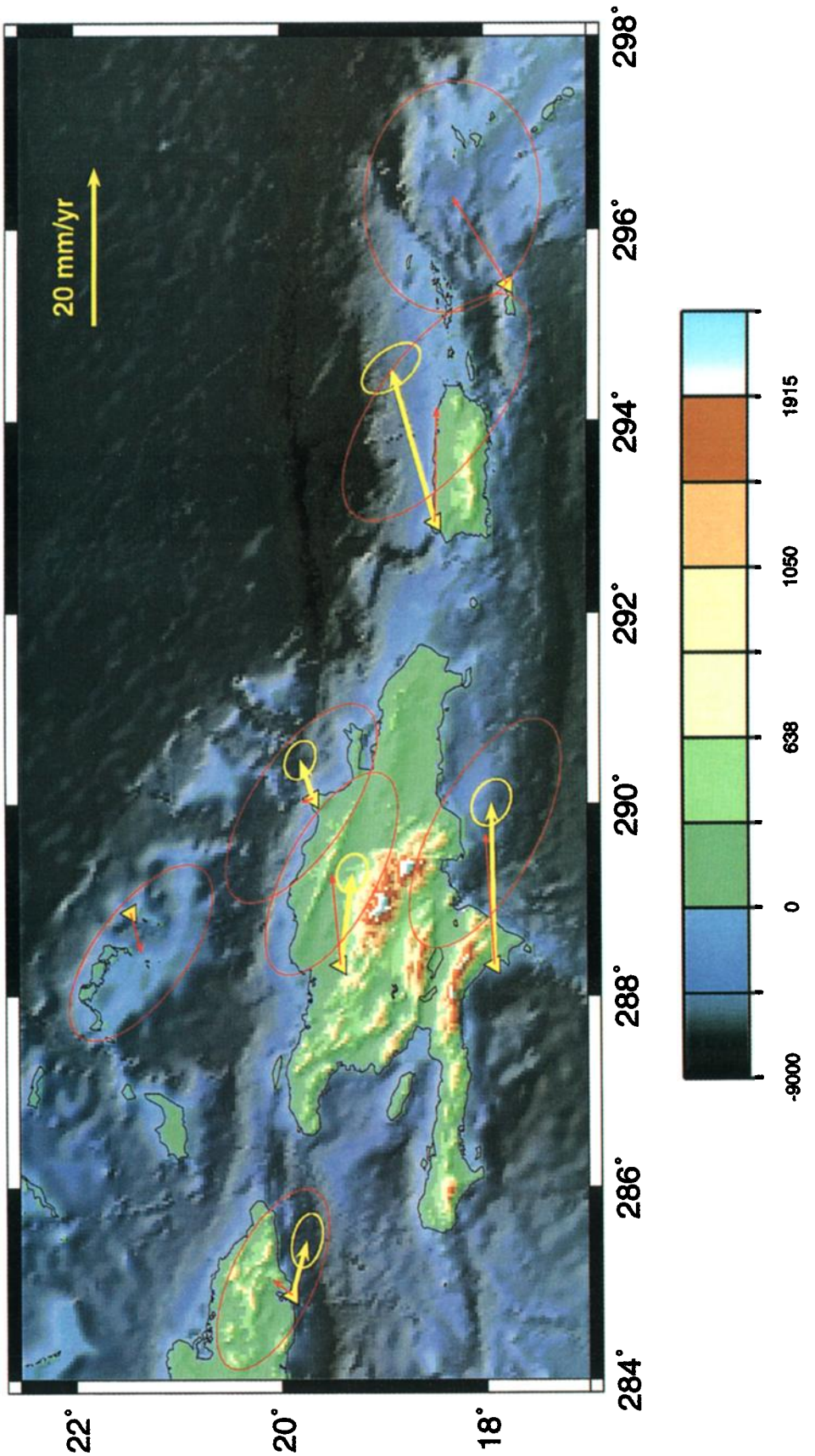

Plate 1. GPS site velocities with respect to Grand Turk (yellow vectors; see Table 6a) and relative to regional North American reference frame (red vectors; see Table 6b), superimposed on a digital bathymetry and land elevation database [*Smith and Sandwell*, 1997]. Error ellipses are two-dimensional, 95% confidence regions (1.73 times two dimensional 1 standard error).

Table 7a. Velocity of ROJO Relative to TURK Based on Data Subsets

	North, mm/yr	East, mm/yr	Vertical, mm/yr
1986-1994	0.8 ± 1.2	21.5 ± 1.8	2.4 ± 6.4
1986-1995	-0.1 ± 1.2	20.4 ± 1.5	-1.0 ± 6.7
1994-1995	-5.2 ± 4.7	14.0 ± 8.0	6.7 ± 15.9
All	0.3 ± 1.0	20.6 ± 1.2	-1.6 ± 4.5

Uncertainties are 1 standard error, based on a model with white measurement noise and random walk monument noise (2.0 mm/√yr) added in quadrature.

1984], perhaps reflecting collision of Hispaniola with the Bahamas Bank [*Mann et al.*, 1995; *Dolan and Wald*, 1997]. The eastward velocity of ROJO is slightly oblique to the trend of the Septentrional fault. Our data are insufficient to address partitioning of strike slip and thrust components in Hispaniola but provide the following constraint. From the measured velocity at ROJO and the azimuth of the surface trace of the Septenrional fault, the fault-normal velocity component in this region is 7.3 ± 1.1 mm/yr (6.7 ± 4.2 in the regional North American reference frame; see Tables 9a and 9b). If all this were accommodated on a single thrust fault (offshore?), if earthquakes on this fault repeated in a characteristic way, and if all the accumulated slip were released in these characteristic events, then we could expect recurrence of 1946-like events (~4 m of convergent seismic slip?) roughly every 600 years. This convergence may influence vertical tectonics of the north coast of the island. Uplifted terraces are well developed there, although the terrace correlated with the last interglacial reef (~125,000 years BP) is only 6-7.5 meters above present mean sea level, implying very slow average uplift rates for this period [*Mann et al.*, 1995].

A complete elastic strain model would include, for each active fault segment, an accurate location, length, strike, dip, sense of slip, slip rate, locking depth, and fraction of aseismic slip. This model should include offshore fault segments that may accommodate oblique or thrust motion. In well-studied regions such as California this kind of problem is relatively well constrained. In the Caribbean region, much less information is available. Ideally, GPS data can help to constrain the necessary parameters.

Table 7b. Velocity of SANA Relative to ITRF-94 Based on Data Subsets

	North, mm/yr	East, mm/yr	Vertical, mm/yr
1991-1994	2.7 ± 5.3	21.6 ± 6.9	5.7 ± 7.8
1991-1996	5.8 ± 3.9	25.5 ± 4.8	17.6 ± 5.1
1994-1996	10.5 ± 6.1	31.4 ± 9.0	35.1 ± 9.3
All	8.2 ± 3.9	24.8 ± 5.3	20.3 ± 6.2

Uncertainties are 1 standard error, based on a model with white measurement noise and random walk noise added in quadrature. Random walk estimates based on data from Richmond, Florida (see text). Because of site location, ITRF coordinate velocities are approximately (better than 3.0 mm/yr) equal to the velocity relative to stable North America.

Table 8. Global Positioning System and Very Long Baseline Interferometry Velocities for St. Croix Relative to North America

	Rate, mm/yr	Azimuth, deg
GPS	12.9 ± 5.6	58 ± 21
VLBI	16.8 ± 0.8	76 ± 8

Azimuth is clockwise from north. Uncertainties are 1 standard error. GPS velocity and error from Table 6b; VLBI data and error from *MacMillan et al.* [1997] and Macmillan (personal communication).

Unfortunately, our data are too sparse to allow us to construct or test detailed models; the number of unknowns greatly exceeds the number of data. Since our vertical velocities are still too noisy to be useful, we have, at most, two horizontal velocity components per site (total of eight data for a plate-boundary-normal transect from Grand Turk to southern Dominican Republic) to constrain a problem with potentially hundreds of unknowns. We therefore approximate the actual velocity field by assuming the system is dominated by a few vertical, parallel, strike- slip faults, completely locked to shallow depth and freely slipping below that depth, and model only the fault-parallel velocity component. Given the sparse data and the similarity between site velocity azimuths and the surface traces of major faults, this approach is probably adequate. However, we emphasize that we are not testing the validity of this model; we assume it. The main parameters and sources of data constraint for these models are given below.

3.1.1. Fault location and type. Only three throughgoing faults are capable of accommodating interplate motion in the vicinity of Hispaniola. Geological

Table 9a. Fault-Parallel and Fault-Perpendicular Velocities Relative to TURK for Dominican Republic Sites

	Parallel, mm/yr	Perpendicular, mm/yr
FRAN	4.1 ± 1.0	3.2 ± 0.9
CAPO	11.4 ± 1.0	2.6 ± 0.8
ROJO	19.3 ± 1.2	7.3 ± 1.1

Based on velocities and errors from Table 6a. The Septentrional fault azimuth is assumed at 110°. Uncertainties account for correlations between north and east error, but do not account for variation in fault azimuth.

Table 9b. Fault Parallel and Perpendicular Velocities Relative to Stable North America for Dominican Republic Sites

	Parallel, mm/yr	Perpendicular, mm/yr
FRAN	-1.1 ± 5.0	1.2 ± 4.1
CAPO	10.5 ± 5.0	4.9 ± 3.7
ROJO	15.3 ± 5.7	6.7 ± 4.2

Based on velocities and errors from Table 6b. The Septentrional fault azimuth is assumed at 110°. Uncertainties account for correlations between north and east error, but do not account for variation in fault azimuth.

mapping or, in the case of offshore faults, bathymetry, sea floor reflectivity and seismicity, define the locus and sense of slip on these faults. Onshore, the Septentrional fault zone in northern Hispaniola and the Enriquillo-Plantain Garden fault zone (hereafter Enriquillo fault) in southern Hispaniola are the dominant features. Both are active, as evidenced by offset Holocene features and Holocene to recent seismicity, and both are left-lateral, strike-slip faults [*Mann and Burke,* 1984; *Taylor et al.*, 1985; *Prentice et al.*, 1993; *Mann et al.*, 1995]. Seismicity offshore to the north suggests the presence of a third major fault, the North Hispaniola fault zone [*Dolan and Wald*, 1997] (Figure 1). Focal mechanisms suggest oblique slip on shallow planes, implying that both strike-slip and dip-slip components are accommodated here [*Molnar and Sykes*, 1969; *Sykes et al.*, 1982; *Calais et al.*, 1992; *Deng and Sykes*, 1995; *Dolan and Wald*, 1997].

The Septentrional fault is the best studied of these faults. It last ruptured north central Dominican Republic about 800 years ago, between 1150 and 1230 A.D., slipping about 5 m horizontally and 2 m vertically [*Prentice et al.*, 1993, 1994]. We tested models where all slip was confined to the Septentrional fault, where slip was partitioned between the Septentrional and either the Enriquillo or North Hispaniola fault, and where slip occurred on all three faults.

3.1.2. Fault slip rate. This is generally unknown, but some constraints are available. In particular, the left-lateral Septentrional fault in northern Dominican Republic appears to accommodate significant slip [*Mann and Burke*, 1984; *Prentice et al.*, 1993]. The preinstrumental historical earthquake record, probably the longest and most complete in the western hemisphere, is also a useful guide. Historical seismicity in southern Hispaniola, including large shocks in 1701, 1751, 1770, and 1910 [*Scherer*, 1912; *Taber*, 1922] is probably related to the Enriquillo fault [*Sykes et al.*, 1982; *Mann et al.*, 1984]. The 1751 and 1770 events were probably $M \sim 8$, based on reports of widespread damage [*Sykes et al.*, 1982]. Earlier events in 1673, 1684, and 1691 caused major damage in both Santo Domingo and Azua on the south coast of Dominican Republic [*Taber*, 1922], suggesting that these may also be related to the Enriquillo fault or its offshore extension. These data suggest that the Enriquillo fault accommodates significant slip.

3.1.3 Fault locking depth. This is estimated from seismic studies. We assume that the nucleation depth of large, shallow, interplate earthquakes approximates the fault locking depth for simple elastic strain models. *Deng and Sykes* [1995] compiled depth estimates for shallow (<60 km) interplate earthquakes based on teleseismic data. Although the number of events near Hispaniola is small, most of these occur near 15 km depth, similar to other areas of continental or transitional crust with normal heat flow. For simplicity we assumed all faults have the same locking depth and tested a range of 5-35 km. The most likely range is 10-20 km, and over this range, locking depth has little impact on results.

For two locked, parallel, infinitely long strike-slip faults in an elastic half-space, the fault-parallel velocity is:

$$v = 1/\pi\{v_{0,a} \tan^{-1}(x/D_a) + v_{0,b} \tan^{-1}[(x - S)/D_b]\} \quad (2)$$

where v is the velocity at perpendicular distance x from the first fault (a); $v_{0,a,b}$ are the far-field velocities of the two faults with locking depths $D_{a,b}$, respectively, and the faults are separated by distance S [*Dixon et al.*, 1995]. The extension to three faults is obvious. We assumed one, two, or three parallel locked faults in our models, varying the relative slip rates and the locking depths in a series of forward models to best match the GPS data. We investigated a range of total far-field slip rates (sum of individual fault slip rates) centered on the measured GPS rate at ROJO relative to stable North America. Thus the main adjustable parameters in the model are one, two, or three slip rates, to be constrained by four data, namely, the fault-parallel velocity components of TURK, FRAN, CAPO, and ROJO.

Best fit models are chosen from simple χ^2 minimization:

$$\chi^2 = \sum_{i=1}^{N} (O_i - C_i)^2/\sigma_i^2 \quad (3)$$

where N is the number of data, O_i is the observed GPS site velocity, C_i is the calculated value from a model, and σ_i is the data error, here taken as the formal velocity error. Even though the models are nonunique, we can define a range of acceptable slip rates, consistent with available data and errors, as follows. Assuming the model is appropriate and velocity errors are normally distributed and accurately estimated, then reduced χ^2 ($=\chi^2/N\text{-}r$), where r is the number of adjustable parameters) will be approximately equal to 1.0. We can assign a probability P to a given χ^2 value, reflecting the probability that random errors result in χ^2 less than or equal to the actual value. In other words, we compare the calculated value to a reference value that is unlikely (say, P = 0.95, or 95% confidence) to be exceeded. $P \approx 0.5$ is the most likely value if the model provides a good fit to the data. χ^2 can also be used to assign confidence limits to estimated parameters. In cases where a model does not provide a good fit to data (i.e., reduced $\chi^2 > 1$), assigned errors can be adjusted accordingly and confidence limits still estimated, but in this case the assumption of appropriate model is violated and the error estimate, and even the meaning of the "best fit" estimate, must be interpreted cautiously. We performed a grid search for locking depths of 5-35 km and slip rates of 0-25 mm/yr for one-, two-, and three-fault models, calculating χ^2 for each model and confidence limits for best fit models.

It is useful to ask whether the improvement in χ^2 for models with two or three faults compared with a model with one fault is more than expected just from adding model parameters (additional degrees of freedom). This can be determined with the F ratio test [*Stein and Gordon*, 1984], which in this case uses χ^2 for the best two-fault models with p adjustable parameters ($p = 2$) and χ^2 for the best single-fault model with r adjustable parameters ($r = 1$), where

$$F = \frac{\left[\chi^2(r) - \chi^2(p)\right] / (p - r)}{\chi^2(p) / (N - p)} \quad (4)$$

and N is the number of data. Using standard statistical tables, we compare the calculated value of F to an expected value at a given probability level to see whether it exceeds some critical value for significance.

Figures 6 and 7, Table 10, and the discussion below summarize the main results of these tests. Given the small number of data, the statistical inferences should be treated with caution. We first test whether observed site velocities are consistent with the single-fault hypothesis; that is, is all slip confined to the Septentrional fault, or are additional faults required by the data? Figure 6 plots χ^2 for a series of single-fault models over a range of fault locking depths. For each depth the far-field slip rate was adjusted to its best fitting value (range 17 to 19 mm/yr). Probability values are calculated for two degrees of freedom (four data minus two adjustable parameters, namely slip rate and locking depth). The velocities do not define a minimum χ^2 over the depth range tested (minimum χ^2 at ~40 km), and no model tested has χ^2 near P = 0.50, implying that a single-fault model poorly fits the data. χ^2 is sufficiently large that we can reject the single-fault model with high confidence. These and other numerical tests also suggest that our data are not appropriate for determining fault locking depth: a minimum χ^2 is not defined over a plausible depth range, defined by the occurrence of shallow crustal earthquakes in the region as well as standard rheological models for the crust and upper mantle. For the remaining discussion we ignore the effect of locking depth, fixing it to the seismic value of 15 km.

Adding 3-5 mm/yr of slip to the North Hispaniola fault improves the fit, reflecting the velocity of the northern site FRAN, but the improvement is not statistically significant. A two-fault model involving the Septentrional and Enriquillo faults improves the fit by a larger amount, significant at 75% but not 90% confidence. Not surprisingly, an excellent fit is obtained with three faults, but, again, we cannot preclude the possibility that the improvement is due to chance-the improvement in χ^2 for the best fitting three-fault model compared to the best fitting single-fault model is significant at 75% but not 90% confidence. Figure 7 shows contoured values of χ^2 for a three-fault model, where slip on the North Hispaniola fault is fixed at 4 mm/yr (its best fitting value) and slip is varied between the Septentrional and Enriquillo faults. Figure 7 illustrates our ability to discriminate the long-term slip rates on these faults with the limited available data (Table 10). The orientation of the ellipse reflects the fact that while there is a trade-off between the velocities of the two faults, there is a stronger constraint on the total slip; the sum of slip rates on the individual faults must equal (or nearly equal) the total plate rate, which is relatively well-constrained. For the best fitting three fault model we obtain slip rates of 8 ± 3 and 8 ± 4 mm/yr for Septentrional and Enriquillo faults, respectively. For the best fitting, two fault model we obtain 13 ± 4 mm/yr for the Septentrional fault and 7 ± 4 mm/yr for the Enriquillo fault.

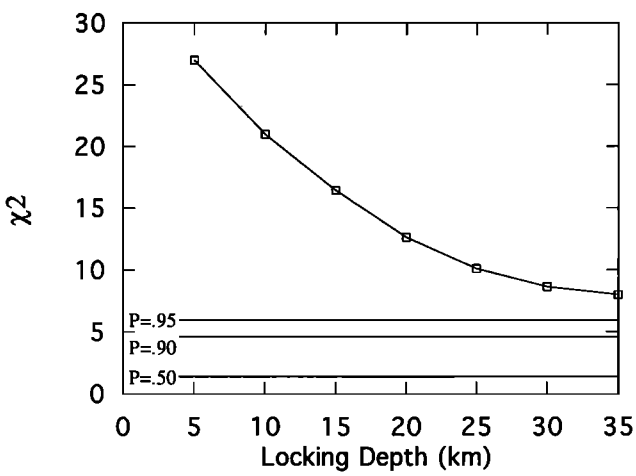

Figure 6. χ^2 (equation (3)) as a function of fault locking depth using the four GPS site velocity data for Hispaniola and Grand Turk (fault-parallel component, Table 9a) and an elastic half-space model (equation (2)) for a single locked fault (Septentrional fault) using local reference frame results. Horizontal lines show probability values P for χ^2 assuming approporiate model.

Combining our best estimate of slip rate on the Septentrional fault (8 mm/yr) and the 800 year elapsed time since the last major earthquake [*Prentice et al.*, 1993] gives 6.4 m of accumulated slip on this fault, consistent with previous estimates of accumulated slip and seismic hazard [*Prentice et al.*, 1993, 1994]. Taking the minimum rate at 1 standard error (4 mm/yr) and the minimum time since the last major earthquake (770 years) gives 3 m of accumulated slip, consistent with a future $M \sim 7$ earthquake, assuming that all the accumulated slip is released in a single event. The Septentrional rate estimate depends strongly on CAPO's velocity, which is based on just two observations, in 1986 and 1994. In view of the importance of refining these numbers for earthquake hazard assessment, additional geodetic measurements, trenching, and other studies in the region are critical.

Figure 8 shows one acceptable model and the GPS data. One important conclusion is that elastic strain effects at ROJO are small, well within the uncertainties of the observations, reflecting its distance from known active faults. Consequently, the velocity of this site may approximate the velocity of the stable interior of the Caribbean plate. Another conclusion is that the Enriquillo fault zone has a relatively fast slip rate, consistent with its history of seismicity over the past three centuries. It may thus constitute a major plate boundary fault. *Rosencrantz and Mann* [1991] and *Mann et al.* [1995] proposed that this fault was essentially continuous with left-lateral faults in Jamaica (Enriquillo-Plantain Garden fault zone) and extends as far west as the Cayman spreading center. *Burke et al.* [1980] proposed 40 km of cumulative post-late Miocene (post-10 Ma), left-lateral offset across Jamaica, for an average rate of 4 mm/yr. Assuming the average rate over the last 10 Myr is representative of present-day rates and assuming the proposed kinematic linkage is correct, the Jamaican rate of left-lateral offset is equivalent to our estimate for the Enriquillo fault zone in Hispaniola within 1 standard error.

3.2. Regional Deformation and Possible Block Rotation

In contrast with ROJO's essentially eastward velocity relative to North America, the velocities of ISAB and CRO1 have a northward component. This apparently precludes models requiring extension and normal faulting across the Puerto Rico Trench [e.g., *Speed and Larue*, 1991] and apparently supports models predicting some convergence between the Caribbean and North American

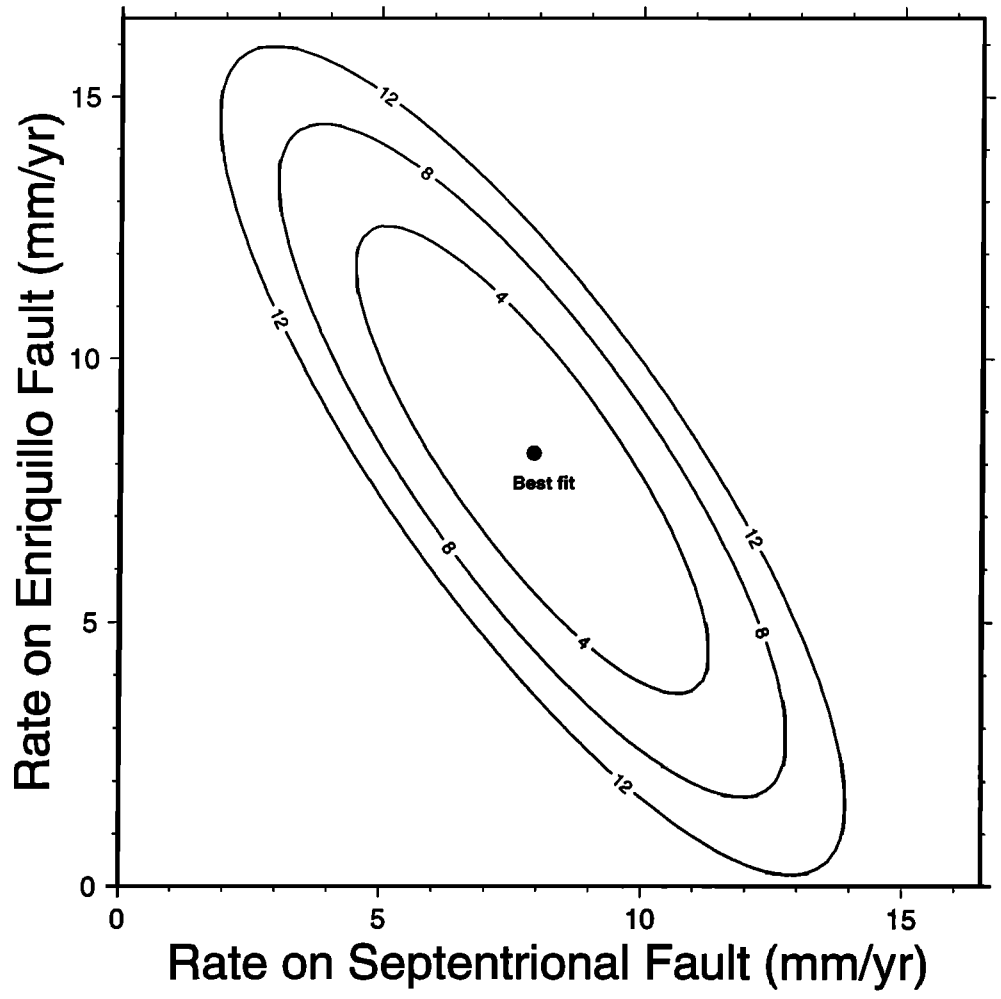

Figure 7. Contours of χ^2 for various slip rates on the Septentrional and Enriquillo faults (0.2 mm/yr grid interval), using local reference frame velocities (Table 6a) and a model with three faults, with slip rate on North Hispaniola fault fixed at 4 mm/yr (best fit value) and locking depth set to 15 km. Contour values correspond approximately to 75%, 90%, and 95% confidence limits for a model with three adjustable parameters (three slip rates) and four data.

plates in this region [*Deng and Sykes*, 1995]. However, are the velocities of these two sites representative of the stable Caribbean plate?

ROJO and ISAB are separated by the Muertos Trough and its possible connection with the east termination of the Enriquillo fault zone (Figure 1). ROJO lies south of any deformation associated with this feature (Figure 1), and, as discussed above, its velocity may approximate stable Caribbean plate. However, ISAB is located north of this putative block boundary. The Muertos Trough reaches depths of 5 km, but its level of present-day activity is not well known. Some authors have argued that the Muertos Trough is a fossil trench, with subduction ending in Oligocene or earlier time [*Malfait and Dinkelman*, 1972; *Burke et al.*, 1978]. However, *Byrne et al.* [1985] describe a *Ms* = 6.7 shallow thrust earthquake in the western Muertos Trough, and interpret the trough as a microplate boundary separating eastern Hispaniola and Puerto Rico from Caribbean lithosphere with a north-dipping subduction zone. Together with a possible south-dipping subduction zone associated with the Puerto Rico trench, these two features would effectively isolate eastern Hispaniola and Puerto Rico from stable Caribbean lithosphere if they are both active. Published seismic reflection data for the Muertos Trough show folded sedimentary layers, but evidence for significant present-day deformation is equivocal [*Ladd et el.*, 1977]. GLORIA side-scan sonar data show young folding in the western Muertos trough, decreasing eastward [*Masson and Scanlon*, 1991]. Seismicity is also more common in the western part of the Trough. Perhaps this asymmetry reflects a connection between the Enriquillo fault zone and the Muertos Trough, with the Muertos Trough accommodating some strike slip motion. Thrust faulting and folding would then be restricted to the right, transpressional step between the Enriquillo fault zone and the Muertos Trough. However, the Muertos Trough is a low angle feature in seismic cross sections, and is not known to accommodate significant strike slip motion. Also, young folding [*Masson and Scanlon*, 1991] seems to extend too far east to be explained by this model. *Deng and Sykes* [1995] suggest that only the western part of the trough is active, because present-day deformation steps north through the active Mona Canyon to link with the

Table 10. Best Fitting Fault Slip Rate Estimates Using Site Velocities Relative to TURK

	Slip Rate, mm/yr
Two Fault Model	
Septentrional Fault	13 ± 3
Enriquillo Fault	7 ± 3
χ^2	6.2
Three Fault Model	
North Hispaniola Fault	4 ± 3
Septentrional Fault	8 ± 3
Enriquillo Fault	8 ± 4
χ^2	0.3

Puerto Rico trench. In this model, ISAB and CRO1 would behave essentially as part of the stable Caribbean plate. A large earthquake in 1918 centered on the Mona Canyon [*Taber*, 1922] is consistent with this model, as is the morphology of the canyon, suggestive of the young normal faulting expected in a left, trans-tensional step in a left-lateral zone of shear.

On the other hand ISAB's velocity azimuth does not match ROJO's, suggesting that ISAB does not represent stable plate interior, and causing problems with the kinematic linkage described above between the Muertos Trough and Puerto Rico trench. The coincidence between ISAB's east-northeast velocity azimuth and the azimuth of earthquake slip vectors in the nearby Puerto Rico trench [*Deng and Sykes*, 1995] suggests that ISAB's velocity does reflect an important aspect of regional tectonics. *Masson and Scanlon* [1991] and *Speed and Larue* [1991] proposed that Puerto Rico and the Virgin Islands behave as a separate rigid block, undergoing counterclockwise rotation associated with Puerto Rico's location in a plate boundary zone in left-lateral shear. In this model the block is bounded on the south by the Muertos Trough, on the north by the Puerto Rico Trench, and on the east by the Anegada Passage fault system (Figure 1). This model requires active convergence across the western Muertos Trough that decreases eastward, and is also consistent with observed normal or right-lateral transtensional faulting in the Passage [*Jany et al., 1990*]. The rotation model could explain ISAB's velocity azimuth (rotated counterclockwise compared with ROJO's) if the axis of block rotation lies west of ISAB. Late Cretaceous lavas [*Fink and Harrison*, 1972], Late Cretaceous to Eocene sedimentary rocks [*Van Fossen et al.*, 1989], and Oligocene to Miocene carbonates [*Reid et al.*, 1991] all show significant post-Eocene to post-Miocene counterclockwise rotation. These data are adequately fit by a model of constant rotation rate at about 1°/Myr, though models involving faster (4°/Myr) Miocene rotation and little or no subsequent rotation have also been proposed [*Reid et al.*, 1991]. However, this model does not explain CRO1's velocity (east-northeast, similar to ISAB) because this site is located south of the proposed block boundary and thus ought to be more representative of stable Caribbean plate interior.

CRO1's velocity (Tables 6b and 8) is slower than ISAB's velocity. This does not seem consistent with a simple block rotation model: the sites are separated by the Anegada Passage, part of the block boundary, and CRO1's velocity seems too slow to represent stable Caribbean plate. CRO1's velocity relative to ISAB is permissive of right-lateral faulting in the Anegada Passage, consistent with the tectonic escape model of *Mauffret and Jany* [1990] for the Puerto Rico-Virgins Islands block. However, this does not explain CRO1's slow velocity relative to ROJO or the Caribbean plate interior. Additional measurements on the numerous small islands in the northeast Caribbean may be required to unravel the complex block tectonics and strain accumulation patterns we suspect characterize this area.

In summary, local tectonic complexities, perhaps related to block rotation, may affect the velocities of ISAB and CRO1. Until the tectonics are better understood, these sites should not be used to model the velocity of the stable Caribbean plate.

3.3. Caribbean - North America Plate Velocity

Euler vectors derived from the GPS horizontal velocities of ROJO and SANA are listed in Table 11, together with several other published Euler vectors. We take two approaches, using ROJO's velocity in both the local and regional frames (Table 6a,b), obtaining similar results. Since the GPS Euler vectors are based on velocities from only two sites (the minimum required), we cannot test for data consistency or plate rigidity.

The new Euler vectors and underlying site velocity data allows us to address several aspects of northern Caribbean tectonics, discussed below in terms of direction and rate of relative motion.

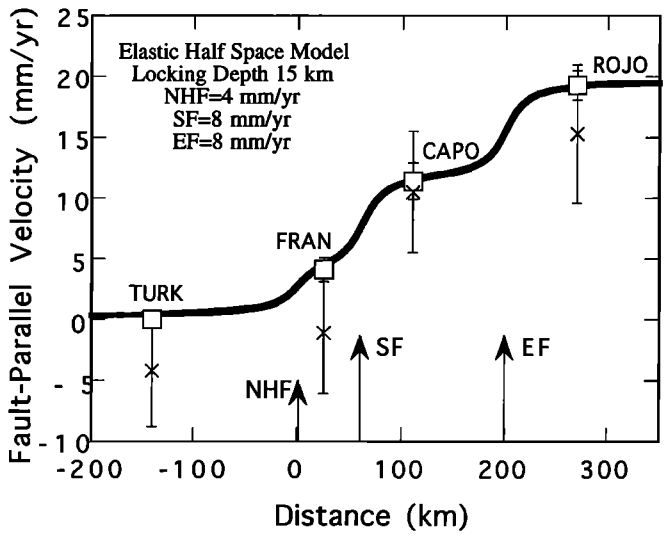

Figure 8. Elastic half-space model (heavy solid curve) corresponding to best fit values in Figure 7 compared to GPS site velocity data for TURK and three Dominican Republic sites (CAPO, FRAN, and ROJO). Squares with small error bars are site velocities relative to TURK (local reference frame, Table 6a), crosses with large error bars are site velocities relative to the regional North American reference frame (Table 6b). Error bars are 1 standard error, after adding random walk noise (see text). Vertical arrows show fault locations; NHF is North Hispaniola fault, SF is Septentrional fault, EF is Enriquillo fault.

Table 11. Some Recent Euler Vectors Describing Caribbean Motion Relative to North America

	Latitude, °N	Longitude, °E	ω, °/m.y.	Error Ellipse			σ_ω, °/m.y.
				σ_{max}	σ_{min}	ζ_{max}	
This study[a]	18.6	107.2	0.36	33.2	5.6	7	0.25
This study[b]	26.4	109.7	0.27	38.0	2.8	3	0.14
DeMets et al [1994]	74.3	153.9	0.105	25.5	2.6	-52	0.03
DeMets [1993][c]	33.6	109.3	0.17	34.2	2.3	-13	0.05
Deng and Sykes[1995]	68.4	-126.3	0.21	-	-	-	-
Calais and Mercier de Lepinay [1993]	33.9	111.0	0.10	-	-	-	-

The Caribbean plate rotates counterclockwise around listed pole. Error ellipse axes σ_{max} and σ_{min} are in degrees, and ζ_{max} is the orientation of the long axis in degrees clockwise from north. Axes are two dimensional 1 standard error; for 95% confidence, multiply by 1.73.

[a] Values are based on the horizontal velocities of SANA and ROJO relative to the regional North American reference frame (Table 6b).

[b] Based on velocities of SANA relative to regional North America reference frame (Table 6b) and ROJO relative to local (TURK) reference frame (Table 6a).

[c] NUVEL - G (geological; model omits all earthquake slip directions).

3.3.1. Direction. One of the outstanding problems in Caribbean tectonics has been reconciling evidence for large, left-lateral offsets associated with the east-west trending Swan and Oriente transform faults [e.g., *Mann and Burke*, 1984] with observations suggesting large-scale crustal convergence, especially near Hispaniola and the Puerto Rico trench. These observations include deep focus earthquakes defining dipping zones analogous to subduction zones, shallow thrust fault earthquakes, folds and thrust faults affecting young sedimentary rocks, thickened crust, and elevated topography [e.g., *Deng and Sykes*, 1995; *Dolan and Wald*, 1997]. Several plate motion models [*Jordan*, 1975; *Stein et al.*, 1988; *DeMets et al.*, 1994] predict essentially east-west motion in the vicinity of Hispaniola, while other models [*Sykes et al.*, 1982; *Deng and Sykes*, 1995] favor more oblique, ENE-WSW relative motion.

The dichotomy between east-west (pure transform) motion and oblique motion with a component of north-south convergence continues to plague interpretations of Caribbean geology and fuel controversy. *Dolan and Wald* [1997] state that overall relative motion between the North American and Caribbean plates is west-southwest rather than pure east-west, while *Russo and Villasenor* [1995, 1997] prefer an east-west direction. *DeMets et al.* [1990] included earthquake focal mechanisms from the Middle America trench in their inversion for global plate motions, predicting eastward motion at relatively slow rate for the Caribbean plate along most of the northern boundary, while *Deng and Sykes* [1995] argued that focal mechanisms from the Middle America Trench should not be used because of partitioning of oblique convergence and consequently biased trench earthquake slip directions. However, *Deng and Sykes* [1995] incorporated focal mechanisms from the Puerto Rico trench, also a region of oblique convergence, leading to predictions of faster Caribbean motion that is obliquely convergent upon North America.

The use of earthquake slip directions for plate or block motion studies necessarily involves selection criteria based in part on a priori models. Space geodetic data can yield information on directions and rates of plate or block motion that is less ambiguous, but is also not free from selection criteria. Determining whether a given geodetic site is located on the stable plate interior, in an elastically straining zone, or on a rotating block is not straightforward, given the complicated tectonics and small number of potential measurement sites on the Caribbean plate interior.

Mann and Burke [1984] attributed evidence for large-scale convergence in and around Hispaniola to a broad right step in an otherwise east-west trending transform zone, leading to transpression within Hispaniola and perhaps nearby offshore. In this model there would be little or no convergence between North America and the stable interior of the Caribbean plate. Our GPS results, specifically the eastward velocity of ROJO with respect to the local North American (TURK) reference frame, provide some support to this view. ROJO's azimuth in this reference frame (N89°E ± 3°; Table 6a) is more easterly than the oblique convergence prediction of *Deng and Sykes* [1995] (N70°E) and more easterly than the NUVEL -1A prediction (N79°E ± 3°). In the regional North American reference frame (Table 6b), ROJO's azimuth is 86 ± 13°, also more easterly than the *Deng and Sykes* [1995] model but equivalent to it within errors. ROJO's azimuth in either reference frame is similar to the eastward extrapolation of a small circle fit through the Swan and Oriente transform faults, an observation supportive of simple models of plate boundary geometry and kinematics involving mainly boundary-parallel, strike-slip motion, at least for the region of Hispaniola westward. The east-northeast azimuths of ISAB and CRO1 suggest this region behaves differently. Perhaps it is decoupled from the stable Caribbean plate interior, e.g., by block rotation or incipient subduction

zones on the north and south margins (Puerto Rioc trench, Muertos Trough). If correct, this may explain the variety of models for Caribbean plate motion; models predicting north-northeast motion incorporate earthquake slip vectors from the Puerto Rico trench. However, this does not explain convergent features in Hispaniola, which more likely reflect the orientation of the Septentrional fault, oblique to our inferred plate motion direction.

A curious aspect of Caribbean tectonics is that although convergence between North and South America increases westward [*Dixon and Mao*, 1997], evidence for convergence along the northern Caribbean plate boundary (e.g., oblique or thrust fault earthquakes) are best developed in the eastern part (Puerto Rico trench, Hispaniola) and are essentially absent to the west along the Swan transform fault. Present day convergence between North and South America in the vicinity of Hispaniola is limited to about 2-4 mm/yr. ROJO's velocity limits the amount of north-south convergence between the Caribbean and North American plates that is accommodated in the vicinity of Hispaniola, irrespective of complexities associated with the oblique Septentrional fault. Convergence not accommodated here must either be accommodated along the southern plate boundary, or by intraplate deformation, or by strike slip motion elsewhere. In the more precise local reference frame, north-south convergence at ROJO is limited to 2.3 mm/yr at 95% confidence (ROJO's north component velocity; see Table 6a). However, in the less precise regional reference frame, up to 8.9 mm/yr of convergence is allowed at 95% confidence (ROJO's north component velocity; see Table 6b). The 95% error ellipse for this velocity estimate includes the azimuth predicted by the *Deng and Sykes* [1995] model. The vector diagram in Figure 9 summarizes the current data constraints and models.

3.3.2. Rate. Rate estimates for the Caribbean plate range from a low of 11 ± 3 mm/yr [*DeMets et al.*, 1994] to a high of 37 ± 5 mm/yr [*Sykes et al.*, 1982]. The GPS data indicate an intermediate value. The NUVEL-1A model [*DeMets et al.*, 1994] predicts 11.4 ± 3.3 mm/yr of eastward motion (N78.8° ± 3.3° E) calculated at ROJO (17.9°N, 71.7°W) compared with our measurement, 20.6 ± 1.2 mm/yr at N89° ± 3° E). The rate difference between the NUVEL-1A model and the GPS measurement is statistically significant at 95% confidence. Minor seismicity south of ROJO (*Sykes et al.*, 1982) may reflect accomodation of a small fraction of Caribbean-North American motion there, making ROJO's velocity a minimum estimate for the rate of Caribbean motion.

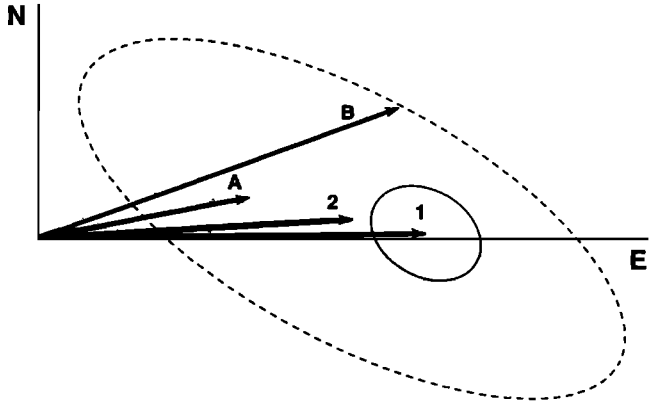

Figure 9. Predicted (model A, *DeMets et al.* [1994]; model B, *Deng and Sykes* [1995]) and observed (1,2, this study) vectors describing ROJO's motion relative to stable North America, assuming ROJO lies on the stable Caribbean plate. Vector 1 is relative to local (TURK) reference frame, vector 2 is relative to regional North American reference frame (Tables 6a and 6b).

Three other aspects of our data support a rate of present-day Caribbean plate motion that is fast compared with the NUVEL-1A model. First, SANA's velocity (Table 6b), based on independent GPS data, is more than twice as fast as the NUVEL-1A model prediction (the directions are similar). We obtain a minimum rate at SANA using just the 1991 and 1994 data; relative to North American that rate is 24.2 ± 6.9 mm/yr. Using data from all three occupations, the minimum rate at 95% confidence is 17.9 mm/yr compared with the NUVEL-1A prediction at SANA of 11.5 ± 3.3 mm/yr.

Second, ISAB's velocity is also relatively fast compared with the corresponding NUVEL 1A prediction. While we do not argue that this site represents the stable interior of the Caribbean plate, its relatively fast rate lends credence to the argument that the Caribbean plate as a whole moves faster with respect to North America than predicted by NUVEL-1A. As with the ROJO result, ISAB's relatively high velocity holds in either definition of the North America reference frame, although in the regional reference frame its velocity is only marginally higher than the NUVEL-1A prediction.

Third, GTMO's velocity is consistent with a Caribbean plate rate that is anomalously fast with respect to NUVEL-1A. This site is within the elastically straining region, and cannot be used to accurately estimate plate motion. However, we can use an elastic model with reasonable parameter values to see if GTMO's velocity is consistent with other GPS data and the fast rate interpretation. GTMO lies on the North American plate, 15 ± 5 km north of the Oriente transform fault. At this location the strike-slip part of the plate boundary is relatively well defined, although some convergent deformation is accommodated to the south in the Santiago Deformed Belt [*Calais and Mercier de Lepinay*, 1991] (Figure 1). If we fit GTMO's velocity to a simple, single-fault, elastic half-space model, we can estimate the fault-parallel component of far-field motion across the Oriente transform fault that is most consistent with GTMO's observed velocity. Assuming that GTMO lies 20 km from the fault and that the fault has a shallow locking depth gives a minimum far-field rate estimate. For a locking depth of 10 km and taking the fault-parallel (east) component of GTMO's velocity as 6.9 ± 1.4 mm/yr (Table 6a), the far-field rate for the best fitting model is 20±4 mm/yr. This is similar to the rate observed at ROJO, again significantly faster than the NUVEL-1A prediction.

Some other data are also consistent with the GPS-derived rate for Caribbean-North America motion. Since most studies (including our own) place the pole of rotation for Caribbean-North America motion far from the Caribbean plate, rate estimates from a wide range of locations along the northern Caribbean boundary can be compared. *White* [1991] estimated a net historical slip rate of 17 to 21

mm/yr across the boundary in Central America, based on measured slip from a few large earthquakes and the earthquake recurrence interval estimated from the historical record. *MacDonald and Holcombe* [1978] estimated spreading rates across the Cayman Rise from limited magnetic anomaly data, obtaining 20 ± 4 mm/yr for the past 2.3 Myr. Later studies suggested lower rates (~15 mm/yr), depending on the time interval averaged and a presumed relation between depth and age [*Rosencrantz et al.*, 1988; *Rosencrantz and Mann*, 1991], but *Rosencrantz* [1995] reinterpreted the data and suggested that the post-early Miocene spreading rate is between 19 and 22 mm/yr, equivalent to the initial result.

This apparent agreement of rate estimates masks a kinematic problem. If spreading across the Cayman Rise occurs today at about 20 mm/yr, simple kinematic arguments suggest that this should "feed" slip on the North Hispaniola and Septentrional faults. Yet our best slip rate estimates on these faults sum to only 12 mm/yr; the full plate rate is obtained only with the addition of ~8 mm/yr on the Enriquillo fault, whose slip is not recorded by Cayman Rise spreading, as pointed out by *Sykes et al.* [1982] and *Rosencrantz and Mann* [1991]. Rate estimates near the limit of various error bounds might solve this problem, for example, Cayman Rise spreading at 17 mm/yr (a plausible value given, variability in published estimates), feeding 11 and 6 mm/yr on the Septentrional and North Hispaniola faults, respectively, with an additional 5 mm/yr on the Enriquillo fault, for a total of 22 mm/yr.

In summary, available GPS data from the CANAPE experiment spanning the northeastern Caribbean plate boundary from Guantanamo Bay, Cuba, to Puerto Rico suggest eastward motion of the Caribbean plate relative to North America at about twice the rate of the NUVEL-1A model prediction. Independent observations at San Andres Island in the western part of the Caribbean plate are consistent with this fast rate, as are some geological and seismic data.

The fact that our measured rate of Caribbean motion is fast with respect to NUVEL-1A is a surprising result. Most other comparisons of plate velocities predicted by NUVEL-1A, representing a geologic average over several million years and global space geodetic measurements averaged over a decade or less, show excellent agreement between the two techniques and timescales, almost always to 5 mm/yr or better [*Smith et al.*, 1990; *Robbins et al.*, 1993; *Robaudo and Harrison*, 1993; *Cazenave et al.*, 1993; *Argus and Heflin*, 1995; *Larson et al.*, 1997]. Below we discuss three explanations for the discrepancy : (1) rapid evolution of Caribbean plate motion, such that velocities on geologic and geodetic time scales differ; (2) anomalous recent activity, biasing the geodetic estimate to fast values; and (3) systematic error in the NUVEL-1A model, biasing the geologic estimate to slow values.

1. Local studies involving North American-Pacific plate relative motion [*Ward*, 1990; *Argus and Gordon*, 1990; *Dixon et al.*, 1991b; *Feigl et al.*, 1993], Caribbean-Cocos relative motion [*Dixon*, 1993], and North America-South America motion [*Dixon and Mao*, 1997] demonstrate that key parts of the plate circuit involving the North America and Caribbean plates have velocities that are similar on geodetic and geologic timescales, within a few millimeters per year. This suggests that rapid evolution of Caribbean motion over the last few million years is not the reason for the discrepancy.

2. The *Ms* = 7.8 1946 Hispaniola earthquake [*Russo and Villasenor*, 1995]) may have induced postseismic effects reflecting viscoelasticity in the mantle. Postseismic effects many decades after major earthquakes have been suggested in several regions [*Pollitz*, 1992; *Pollitz and Sacks*, 1994], and could lead to anomalously fast rates, since they tend to be in the direction of plate motion and seismic slip. Such effects should fall off with distance from the epicenter, so the fast rates at ISAB, GTMO and SANA would seem to rule out this explanation. *Pollitz and Dixon* [1998] describe the results of viscoelastic modeling that suggest the effects on measured site velocities in Dominican Republic are less than about 2 mm/yr and thus cannot account for the discrepancy.

3. We are left with the third explanation, namely that systematic error in the NUVEL-1A model causes it to mismodel . Caribbean plate velocity. NUVEL-1A apparently underestimates the rate of Caribbean-North American motion, probably owing to weaknesses in the relevant data. These data include earthquake slip directions from the Middle America Trench that were assumed to record Cocos-Caribbean convergence direction, earthquake slip directions from the Lesser Antilles trench used to constrain the Caribbean-South American slip direction, and spreading rates and slip directions from the Caribbean-North American plate boundary. Of these observations, only the slip directions from the eastern Swan Islands transform fault, which locally accommodates strike-slip motion between the Caribbean and North American plates [*Rosencrantz and Mann*, 1991] unambiguously record motion of adjacent stable plate interiors. The remaining observations are subject to a variety of systematic biases. For example, oblique convergence between the Cocos and Caribbean plates along the Middle America Trench appears to be accommodated via essentially trench-normal convergence combined with trench-parallel, strike-slip motion within the Central American volcanic arc [*White*, 1991; *White and Harlow*, 1993]. Earthquake slip directions from shallow thrust earthquakes along this portion of the trench may be more representative of relative motion between the Cocos plate and the forearc than they are of Cocos-Caribbean relative motion [*Deng and Sykes*, 1995]. One point in favor of this explanation is that the GPS Euler vectors are in better agreement with a NUVEL-based Euler vector ("NUVEL-G", for geological) that omits all local earthquake data [*DeMets et al.*, 1993] compared to the standard NUVEL-1A model (Table 11). In a future paper we will discuss these arguments in detail, present a revised circum-Caribbean plate kinematic model incorporating the GPS velocities, and discuss implications for present-day global plate motions (C. DeMets et al., manuscript in preparation, 1998).

4. Conclusions

1. GPS observations spanning a decade have been analyzed to investigate plate motion and crustal deformation in the northeastern Caribbean. Data quality and formats evolved considerably over this period and satellite orbit knowledge for the older data is weak

compared with newer data, but the older data are important for resolving slow rates of crustal motion in the region. Data of this vintage should be carefully archived for future research; our studies point to some gaps, especially in older tracking data.

2. GPS data from three sites in Dominican Republic combined with simple elastic strain accumulation models and geologic and seismic evidence suggest some constraints on strain partitioning. Models where all slip is confined to the Septentrional fault poorly fit the velocity data, implying that the plate boundary cannot be confined exclusively to this fault. We infer that the Septentrional fault accommodates 8 ± 3 mm/yr of left-lateral slip or 25%-55% of the total plate rate, about the same amount as the Enriquillo fault (8 ± 4 mm/yr), the locus of major historical earthquakes. A small amount of strike-slip motion (4 ± 3 mm/yr) may be accommodated along the North Hispaniola fault, consistent with oblique slip earthquakes offshore.

3. GPS data at ROJO suggest that the Caribbean plate moves east with respect to North America at about twice the rate predicted by the NUVEL-1A plate motion model. The GPS data do not require oblique convergence of the Caribbean plate against North America, but neither are they able to preclude it, given current error levels.

4. The observations of relatively fast plate motion and relatively fast slip rates on individual faults suggest that seismic risk estimates based on older, slower rate estimates may underestimate actual seismic hazard. Refining the slip rate estimates on individual faults, including offshore faults, should be a high priority in future studies.

5. Additional geodetic sites, more accurate geodetic site velocities, and more sophisticated strain models are required to resolve critical details related to the locations, orientations, and slip rates of active fault segments; the nature of strain accumulation; the role of block rotations; and the direction of plate motion in the northeastern Caribbean.

Acknowledgments. The first Caribbean GPS observations were sponsored by NASA's Geodynamics Program. The 1994 observations were sponsored by NSF grants to C. DeMets, T. Dixon, P. Jansma, and P. Mann, and a grant from INSU, Tectoscope-Positionnement program to Calais. The 1995 observations were made with funding from NASA to T. Dixon and P. Jansma and receivers owned by the University of Wisconsin. We are indebted to numerous people at JPL, UNAVCO, universities, geodetic observatories, and elsewhere over the last decade for planning and carrying out these observations and for helping us "track down" GPS tracking data. We especially thank those involved in the planning and execution of the 1986 campaign, all of whom broke new ground, including Roger Bilham, Carl Bowin, Steve Dinardo, Gilian Foulger, Matt Golombek, Elsa Hernandez, James Joyce, Bill Melbourne, Nick Renzetti, Chris Rocken, Bruce Stephens, Cathy Thornton, Chuck Vegas, and Tom Yunck. We thank Glen Mattioli for assistance with the 1994 and later observations in Puerto Rico, Ailin Mao for providing the maximum likelihood noise estimates in advance of publication, John Langbein for MLE software, and Kristine Larson for helpful discussions on bias fixing. Many figures in this paper were produced with Generic Mapping Tools (GMT) software [*Wessel and Smith*, 1995]. Walter Smith provided new digital bathymetry data for the Caribbean region in a GMT-compatible format. We also thank IGS and the global geodetic community who provided high-quality global tracking data for analysis of 1994 and later data, Jeff Freymueller who provided the 1991 data for San Andres Island and corresponding tracking data, and Yehuda Bock who provided several papers in advance of publication. Bob King, Lynn Sykes, and Jim Kellogg provided thoughtful reviews that greatly improved the manuscript. UTIG contribution 1300.

References

Argus, D. F., and R. G. Gordon, Pacific-North America plate motion from very long baseline interferometry compared with motion inferred from magnetic anomalies, transform faults, and earthquake slip vectors, *J. Geophys. Res., 95*, 17,315-17,324, 1990.

Argus, D. F., and R. G. Gordon, Tests of the rigid-plate hypothesis and bounds on intraplate deformation using geodetic data from very long baseline interferometry, *J. Geophys. Res., 101*, 13,555-13,572, 1996.

Argus, D. F., and M. B. Heflin, Plate motion and crustal deformation estimated with geodetic data from the Global Positioning System, *Geophys. Res. Lett., 22*, 1973-1976, 1995.

Blewitt, G., M. B. Heflin, F. H. Webb, U. J. Lindqwister, and R. P. Malla, Global coordinates with centimeter accuracy in the International Terrestrial Reference Frame using GPS, *Geophys. Res. Lett, 19*, 853-856, 1992.

Boucher, C., Z. Altamimi and L. Duhem, Results and analysis of the ITRF93, *Tech. Note 18*, 313 pp, Int. Earth Rotation Serv., Paris, France,1994.

Boucher, C., Z. Altamimi, M. Feissel, and P. Sillard, Results and analysis of the ITRF-94, *Tech. Note 20*, 191 pp. Int. Earth Rotation Serv., Paris, France, 1996.

Bryant, M. A., and C. E. Noll, *NASA Space Geodesy Program, Catalog of Site Information, NASA TM-4482*, 655 pp., 1993.

Burke, K. P., J. Fox, and A.M. Celal Sengor, Bouyant ocean floor and the evolution of the Caribbean, *J. Geophys. Res., 83*, 3949-3954, 1978.

Burke, K. P., J. Grippi, and A.M. Celal Sengor, Neogene structures in Jamaica and the tectonic style of the Caribbean plate boundary zone, *J. Geol.*, 88, 375-386, 1980.

Byrne, D. B., G. Suarez, and W. R. McCann, Muertos Trough subduction-microplate tectonics in the northern Caribbean, *Nature*, 317, 420-421, 1985.

Calais, E., and B. Mercier de Lepinay, From transtension to transpression along the northern Caribbean plate boundary off Cuba: Implications for the recent motion of the Caribbean plate, *Tectonophysics, 116*, 329-350, 1991.

Calais, E., and B. Mercier de Lepinay, Semiquantitative modeling of strain and kinematics along the Caribbean-North American strike slip plate boundary zone, *J. Geophys. Res., 98*, 8293-8308, 1993.

Calais, E., N. Bethoux, and B. Mercier de Lepinay, From transcurrent faulting to frontal subduction: A seismotectonic study of the northern Caribbean plate boundary from Cuba to Puerto Rico, *Tectonics, 11*, 114-123, 1992.

Case, J., and T. Holcombe, Geologic map of the Caribbean region, *U S. Geol. Surv. Misc. Invest. Map, I-1100*, 1980.

Cazenave, A., P. Gegout, L. Soudarin, K. Dominh, F. Barlier, P. Exertier, and Y. Boudon, Geodetic results from Lageos 1 and DORIS satellite data, in *Contributions of Space Geodesy to Geodynamics, Crustal Dynamics, Geodyn. Ser.*, vol. 23. edited by D. Smith and D. Turcotte., pp. 81-98. AGU, Washington, D.C., 1993.

Chen, G. and T. A. Herring, Effects of atmospheric azimuthal asymetry on the analysis of space geodetic data, *J Geophys. Res., 102*, 20,489-20,502, 1997.

DeMets, C., Earthquake slip directions and estimates of present-day plate motions, *J. Geophys. Res.*, 98, 6703-6714, 1993.

DeMets, C., R. G. Gordon, D. F. Argus, and S. Stein, Current plate motions, *Geophys. J. Int., 101*, 425-478, 1990.

DeMets, C., R. G. Gordon, D. F. Argus, and S. Stein, Effect of recent revisions to the geomagnetic time scale on estimates of current plate motion, *Geophys. Res. Lett., 21*, 2191-2194, 1994.

Deng, J., and L. R. Sykes, Determination of Euler pole for contemporary relative motion of Caribbean and North American plates using slip vectors of interplate earthquakes, *Tectonics, 14*, 39-53, 1995.

Dewey, J. D., and G. Suarez, Seismotectonics of Middle America, in *Neotectonics of North America*, edited by D. B. Slemmons, M. D. Zoback, and D. Blackwell, pp. 309-321, Geol. Soc. of Am., Boulder, Colo., 1991.

Dixon, T. H., GPS measurement of relative motion of the Cocos and Caribbean plates and strain accumulation across the middle America trench, *Geophys Res. Lett., 20*, 2167-2170, 1993.

Dixon, T. H., and A. Mao, A GPS estimate of relative motion between North and South America, *Geophys. Res. Lett., 24*, 535-538, 1997.

Dixon, T. H., and S. Kornreich Wolf, Some tests of wet tropospheric calibration for the Casa Uno Global Positioning System Experiment, *Geophys. Res. Lett., 17*, 203-206, 1990.

Dixon, T. H., G. Gonzalez, S. M. Lichten, and E. Katsigris, First epoch geodetic measurements with the Global Positioning System across the northern Caribbean plate boundary zone, *J. Geophys. Res., 96*, 2397-2415, 1991a.

Dixon, T. H., G. Gonzalez, S. M. Lichten, D. M. Tralli, G. Ness, and P. Dauphin, A preliminary determination of Pacific-North America relative motion in the southern Gulf of California using the Global Positioning System, *Geophys Res. Lett., 18*, 861-864, 1991b.

Dixon, T. H., S. Robaudo, J. Lee, and M. C. Reheis, Constraints on present-day Basin and Range deformation from space geodesy, *Tectonics, 14*, 755-772, 1995.

Dixon, T. H., A. Mao, and S. Stein, How rigid is the stable interior of the North American plate, *Geophys Res. Lett, 23*, 3035-3038, 1996.

Dixon, T. H. A. Mao, M. Bursik, M. Heflin, J. Langbein, R. Stein, and F. Webb, Continuous monitoring of surface deformation at Long Valley Caldera, California, with GPS, *J. Geophys. Res., 102*, 12,017-12,034, 1997.

Dolan, J. F., and D. J. Wald, Comment on "The 1946 Hispaniola earthquakes and the tectonics of the North America-Caribbean plate boundary zone, northeastern Hispaniola" by R. M. Russo and A. Villasenor, *J. Geophys. Res., 102*, 785-792, 1997.

Dziewonski, A. M., and J. H. Woodhouse, An experiment in systematic study of global seismicity in centroid moment solutions for 201 moderate to large earthquakes of 1981, *J. Geophys. Res., 88*, 3247-3271, 1983.

Feigl, K., et al., Space geodetic measurement of crustal deformation in central and southern California, 1984-1992, *J. Geophys. Res., 98*, 21,677-21,712, 1993.

Fink, L. K., and C. G. A. Harrison, Paleomagnetic investigations of selected lava units on Puerto Rico, *Proceedings, 6th Caribbean Geological Conference*, p. 379, Margarita, Venezuela, 1972.

Frankel, A., A composite focal mechanism for microearthquakes along the northeastern border of the Caribbean plate, *Geophys. Res. Lett., 9*, 511-514, 1982.

Heflin, M., et al., Global geodesy using GPS without fiducial sites, *Geophys. Res. Lett., 19*, 131-134, 1992.

Holcombe, T. L., P. R. Vogt, J. E. Mathews, and R. R. Murchison, Evidence for sea floor spreading in the Cayman Trough, *Earth Planet. Sci. Lett., 20*, 357-371, 1973.

Jany, I., K. M. Scanlon, and A. Mauffret, Geological interpretation of combined Seabeam, Gloria, and seismic data from Anegada Passage (Virgin Islands, North Caribbean), *Mar. Geophys. Res., 12*, 173-196 1990.

Johnson, H. O., and D. C. Agnew, Monument motion and measurement of crustal velocities, *Geophys. Res. Lett., 22*, 2905-2908, 1995.

Jordan, T. H., The present-day motions of the Caribbean plate, *J. Geophys. Res., 80*, 4433-4439, 1975.

Kellogg, J. N., and T. H. Dixon, Central and South America GPS geodesy-CASA Uno, *Geophys. Res. Lett., 17*, 195-198, 1990.

Ladd, J. W., J. L. Worzel, and J. S. Watkins, Multifold seismic reflection records from the northern Venezuela basin and north slope of Muertos Trench, in *Island Arcs, Deep Sea Trenches and Back-Arc Basins, Maurice Ewing Ser.*, vol. 1, edited by M. Talwani and W.C. Pitman III, pp., 41-56, AGU, Washington, D.C., 1977.

Langbein, J., and H. Johnson, Correlated errors in geodetic time series: Implications for time-dependent deformation, *J. Geophys. Res., 102*, 591-603, 1997.

Larson, K. M., J. T. Freymueller, and S. Philipsen, Global plate velocities from the Global Positioning System, *J. Geophys. Res., 102*, 9961-9981, 1997.

Larue, D. K., J. Joyce, and H. F. Ryan, Neotectonics of the Puerto Rico Trench: Extensional tectonism and forearc subsidence, in *Transactions, 12th Caribbean Geological Conference*, edited by D. Larue and G. Draper, pp. 231-247, Miami Geol. Soc., Miami, Fla., 1990.

Lichten, S. M., Estimation and filtering for high precision GPS applications, *Man. Geod., 15*, 159-176, 1990.

Lisowski, M., J. C. Savage, and W. H. Prescott, The velocity field along the San Andreas fault in central and southern California, *J. Geophys. Res., 96*, 8369-8389, 1991.

Lundgren, P. R., and R. M. Russo, Finite element modeling of crustal deformation in the North American-Caribbean plate boundary zone, *J. Geophys. Res., 101*, 11,317-11,328, 1996.

MacDonald, K. C., and T. L. Holcombe, Inversion of magnetic anomalies and sea-floor spreading in the Cayman Trough, *Earth Planet. Sci. Lett., 40*, 407-414, 1978.

MacMillan, D. S., C. Ma, J. W. Ryan, and T. A. Clark, VLBI measurement of Caribbean plate motion, *EOS: Trans. Am. Geophys. U, 78*, S114, 1997.

Malfait, B., and M. G. Dinkelman, Circum-Caribbean tectonic and igneous activity and the evolution of the Caribbean plate, *Geol. Soc. Am. Bull., 83*, 251-272, 1972.

Mann, P., and K. Burke, Neotectonics of the Caribbean, *Rev. Geophys., 22*, 309-362, 1984.

Mann, P., P. McLaughlin, and C. Cooper, Geology of the Azua and Enriquillo basins, Dominican Republic, 2, Structure and tectonics, in *Geologic and Tectonic Development of the North America-Caribbean Plate Boundary in Hispaniola*, edited by P. Mann, G. Draper, and J. F. Lewis, *Spec. Pap. Geol. Soc. Am., 262*, 367-389, 1991.

Mann, P., F.W. Taylor, R. Edwards, and T.L. Ku, Actively evolving microplate formation by oblique collision and sideways motion along strike-slip faults: An example from the northeastern Caribbean plate margin, *Tectonophysics 246*, 1-69, 1995.

Masson, D. G., and K. M. Scanlon, The neotectonic setting of Puerto Rico, *Geol. Soc. Am. Bull., 103*, 144-154, 1991.

Mauffret, A., and I. Jany, Collision et tectonique d'expulsion le long de la frontiere Nord Caribe, *Oceanol. Acta, 10*, 97-116, 1991.

Molnar, P., and L. R. Sykes, Tectonics of the Caribbean and Middle America regions from focal mechanisms and seismicity, *Geol. Soc. Am. Bull., 80*, 1639-1684, 1969.

Pollitz, F., Postseismic relaxation theory on the spherical earth, *Bull. Seismol. Soc. Am , 82*, 422-453, 1992.

Pollitz, F., and S. Sacks, Fault model of the 1891 Nobi

earthquake from historic triangulation and leveling, *J. Phys. Earth, 42*, 1-43, 1994.

Pollitz, F., and T. H. Dixon, GPS measurements across the northern Caribbean plate boundary zone: Impact of postseismic relaxation following historic earthquakes, *Geophys. Res. Lett.*, in press, 1998.

Prentice, C., P. Mann, F. W. Taylor, G. Burr, and S. Valastro, Paleoseismicity of the North American plate boundary (Septentrional fault), Dominican Republic, *Geology, 21*, 49-52, 1993.

Prentice, C., P. Mann, G. Burr, and L. Pena, Timing and size of the most recent earthquake along the central Septentrional fault, Dominican Republic, *US. Geol. Surv. Open File Rep., 94-568*, 158 pp., 1994.

Reid, J.A., P.W. Plumley, and J. H. Schellekens, Paleomagnetic evidence for Late Miocene counterclockwise rotation of north coast carbonate sequence, Puerto Rico, *Geophys. Res. Lett., 18*, 565-568, 1991.

Robaudo, S., and C. G. A. Harrison, Plate tectonics from SLR and VLBI data, in *Contributions of Space Geodesy to Geodynamics: Crustal Dynamics, Geodyn. Ser.*, vol. 23, edited by D.E. Smith and D.L. Turcotte, pp. 51-71, AGU, Washington, D.C., 1993.

Robbins, J.W., D.E. Smith, and C. Ma, Horizontal crustal deformation and large scale plate motins inferred from space geodetic techniques, in *Contributions of Space Geodesy to Geodynamics: Crustal Dynamics, Geodyn. Ser.*, vol. 23, edited by D.E. Smith and D.L. Turcotte, pp. 21-36, AGU, Washington, D.C., 1993.

Rosencrantz, E., Opening of the Cayman Trough and evolution of the northern Caribbean plate boundary, *Geol. Soc. Am., Abstr. Programs, 27*, A-153, 1995.

Rosencrantz, E., and P. Mann, SeaMarc-II mapping of transform faults in the Cayman Trough, Caribbean Sea, *Geology, 19*, 690-693, 1991.

Rosencrantz, E., M. I. Ross, and J. G. Sclater, Age and spreading history of the Cayman Trough as determined from depth, heat flow, and magnetic anomalies, *J. Geophys. Res., 93*, 2141-2157, 1988.

Russo, R. M., and A. Villasenor, The 1946 Hispaniola earthquakes and the tectonics of the North America-Caribbean plate boundary zone, northeastern Hispaniola, *J. Geophys. Res., 100*, 6265-6280, 1995.

Russo, R. M., and A. Villasenor, Reply, *J. Geophys. Res., 102*, 793-802, 1997.

Scherer, J., Great earthquakes in the island of Haiti, *Bull. Seismol. Soc. Am., 2*, 161-180, 1912.

Smith, D. E., R. Kolenkiewicz, P. J. Dunn, J. W. Robbins, M. H. Torrence, S. Klosko, R. G. Williamson, E. C. Pavlis, N. B. Douglas, and S. K. Fricke, Tectonic motion and deformation from satellite laser ranging to LAGEOS, *J. Geophys Res., 95*, 22,013-22041, 1990.

Smith, W. H. F., and D. T. Sandwell, Global sea floor topography from satellite altimetry and ship depth soundings, *Science, 277*, 1956-1961, 1997.

Speed, R. C., and D. K. Larue, Extension and transtension in the plate boundary zone of the northeastern Caribbean, *Geophys. Res Lett., 18*, 573-576, 1991.

Stein, S. and R. G. Gordon, Statistical tests of additional plate boundaries from plae motion inversions, *Earth Planet Sci. Lett., 69*, 401-412, 1984.

Stein, S., C. DeMets, R. G. Gordon, J. Brodholt, D. Argus, J. F. Engeln, P. Lundgren, C. Stein, D. Wiens, and D. Woods, A test of alternative Caribbean plate relative motion models, *J. Geophys. Res., 93*, 3041-3050, 1988.

Sykes, L. R., W. R. McCann, and A. L. Kafka, Motion of the Caribbean plate during the last 7 million years and implications for earlier Cenozoic movements, *J. Geophys. Res., 87*, 10,656-10,676, 1982.

Taber, S., The great fault troughs of the Antilles, *J. Geol., 30*, 89-114, 1922.

Taylor, F. W., P. Mann, S. Valastro, and K. Burke, Stratigraphy and radiocarbon dating of a subaerially exposed Holocene coral reef, Dominican Republic, *J. Geol., 93*, 311-332, 1985.

Van Fossen, M. C., J. E. T. Channell, and J. H. Schellekens, Paleomagnetic evidence for Tertiary anticlockwise rotation in southwest Puerto Rico, *Geophys. Res. Lett., 16*, 819-822, 1989.

Ward, S. N., Pacific-North America plate motions: New results from very long baseline interferometry, *J. Geophys. Res., 95*, 21,965-21,981, 1990.

Wdowinski, S., Y. Bock, J. Zhang, P. Feng, and J. Genrich, Southern California permanent GPS geodetic array: Spatial filtering of daily positions for estimating coseismic and postseismic displacements induced by the 1992 Landers earthquake, *J. Geophys. Res., 102*, 18,057-18,070, 1997.

Wessel, P., and W. H. F. Smith, New version of generic mapping tools released, *Eos Trans. AGU., 76*, 329, 1995.

White, R. A., Tectonic implications of upper-crustal seismicity in Central America, *in Neotectonics of North America*, edited by D. B. Slemmons, M. D. Zoback, and D. Blackwell, pp. 323-338, Geol. Soc. of Am., Boulder, Colo., 1991.

White, R. A., and D. H. Harlow, Destructive upper-crustal earthquakes of Central America since 1900, *Bull. Seismol. Soc. Am., 83*, 1115-1142, 1993.

Zhang, J., Y. Bock, H. Johnson, P. Feng, S. Williams, J. Genrich, S. Wdowinski, and J. Behr, Southern California permanent GPS geodetic array: Error analysis of daily position estimates and site velocities, *J. Geophys. Res., 102*, 18,035-18,055, 1997.

Zumberge, J. F., M. Heflin, D. Jefferson, M. Watkins, and F. Webb, Precise point positioning for efficient and robust analysis of GPS data from large networks, *J. Geophys. Res., 102*, 5005-5017, 1997.

E. Calais, Institue de Geodynamique, Centre National de la Recherche Scientifique, Verriares-le-Buisson, France.

C. DeMets, Department of Geology and Geophysics, University of Wisconsin, Madison, WI 53706.

T.H. Dixon and F. Farina, Rosenstiel School of Marine and Atmospheric Sciences, University of Miami, 4600 Rickenbacker Causeway, Miami, FL 33149. (e-mail: tim @corsica.rsmas.miami.edu)

P. Jansma, Department of Geology, University of Puerto Rico, Mayaguez, PR, 00681-5000.

P. Mann, Institute for Geophysics, University of Texas, 4412 Spicewood Springs Rd., Austin, TX, 78759-8500.

(Received March 25, 1997; revised October 28, 1997; accepted December 4, 1997.)